



# Australian Journal of Earth Sciences

An International Geoscience Journal of the Geological Society of Australia

ISSN: (Print) (Online) Journal homepage: <https://www.tandfonline.com/loi/taje20>

## Foliation boudinage structures in the Mount Isa Cu system

B. J. Williams, T. G. Blenkinsop, R. Lilly, M. P. Thompson & P. Ila'ava

To cite this article: B. J. Williams, T. G. Blenkinsop, R. Lilly, M. P. Thompson & P. Ila'ava (2023): Foliation boudinage structures in the Mount Isa Cu system, Australian Journal of Earth Sciences, DOI: [10.1080/08120099.2022.2153384](https://doi.org/10.1080/08120099.2022.2153384)

To link to this article: <https://doi.org/10.1080/08120099.2022.2153384>



© 2023 The Author(s). Published by Informa UK Limited, trading as Taylor & Francis Group.



[View supplementary material](#)



Published online: 30 Jan 2023.



[Submit your article to this journal](#)






[View related articles](#)



[View Crossmark data](#)

## Foliation boudinage structures in the Mount Isa Cu system

B. J. Williams<sup>a</sup> , T. G. Blenkinsop<sup>a</sup> , R. Lilly<sup>b</sup> , M. P. Thompson<sup>c</sup> and P. Ila'ava<sup>d</sup>

<sup>a</sup>School of Earth and Environmental Sciences, Cardiff University, Cardiff, UK; <sup>b</sup>Department of Earth Sciences, The University of Adelaide, Adelaide, Australia; <sup>c</sup>Avebury Metals, Avebury Nickel Mine, Zeehan, Australia; <sup>d</sup>Mount Isa Mines, Glencore Zinc, Mount Isa, Australia

### ABSTRACT

Small-scale foliation boudinage structures occur in rocks that were sampled in drill core from the Mount Isa Cu deposit, northwest Queensland. The necks of foliation boudinage structures plunge gently to the north and south as a result of layer normal shortening and layer parallel extension of the steeply west-dipping Urquhart Shale. Detailed petrographic analysis of the foliation boudinage structures has identified an initial rim of quartz and dolomite, followed by infill and replacement by pyrrhotite and minor chalcopyrite. Foliation boudinage structures formed after dolomitisation and silicification of the shale. They occur most commonly in the unaltered Urquhart Shale where the anisotropy and homogeneity provided by the shale layering is still intact. Infilling of the structures occurred during protracted silica-dolomite alteration, pyrrhotite and chalcopyrite mineralisation. The paragenesis of the foliation boudinage structures is consistent with the established paragenesis of the main Cu mineralisation. Foliation boudinage structures formed over the period from shortening during D4a through to the main Cu mineralisation during D4b west-northwest-east-southeast sinistral-reverse shortening. The timing of foliation boudinage is consistent with a current kinematic model for the Mount Isa system.

### KEY POINTS

1. First record of foliation boudinage structures at Mount Isa.
2. Foliation boudinage structures with sulfide-dominated infills.
3. Foliation boudinage structures formed as a result of progressive deformation from a D4a dextral-reverse through to D4b sinistral-reverse slip.
4. Foliation boudinage structures are associated with the timing and kinematics of Cu mineralisation at Mount Isa.

### ARTICLE HISTORY

Received 3 October 2022  
Accepted 20 November 2022

### KEYWORDS



Mount Isa; Proterozoic; foliation boudinage structures; Cu mineralisation; pyrrhotite; petrography; drill core; deformation; ore deposit

## Introduction

The world-class Mount Isa Cu and Pb–Zn deposit is located in the Mount Isa Inlier of northwest Queensland (Figure 1). Mount Isa Mine is the second-largest copper producer in Australia, producing approximately 6.5 Mt of ore per year up to 3.3 wt% Cu, with an estimated pre-mining total comprising 150 Mt at 7 wt% Zn and 6 wt% Pb, and 255 Mt at 3.3 wt% Cu (Glencore, 2022; Large *et al.*, 2002, 2005; Potgieter, 2015). The Pb–Zn orebodies are generally close to the surface (Figure 2), where stratiform galena and sphalerite are hosted within dolomitic layers (Bell *et al.*, 1988; Cave *et al.*, 2020). The breccia dominated Cu ore bodies are located within a silica-dolomite alteration halo and occupy a deeper level in the Mount Isa system (Bell *et al.*, 1988; Perkins, 1984; Swager, 1985). The Cu orebodies

are typically discordant to bedding and interdigitate with the Pb–Zn orebodies (Bell *et al.*, 1988; Cave *et al.*, 2020; Perkins, 1984; Swager, 1985; Swager *et al.*, 1987).

The details of the Mount Isa Cu ore bodies have been subjected to some recent revisions. Bell *et al.* (1988), Davis (2004), Miller (2007), Perkins (1984) and Swager (1985) have all argued for Cu emplacement at a late stage in a complex deformation history. However, even within these previous models there are different interpretations for the controls on Cu ore body orientations and relative timings (*e.g.* Miller, 2007; Perkins, 1984). Early studies suggest a Cu mineralisation event during an early phase of D4 deformation (Bell *et al.*, 1988; Perkins, 1984), however, Miller (2007) identified that the bulk of Cu mineralisation occurred during an additional later phase of the main D4 event. The relative

CONTACT B. J. Williams  [williamsb39@cardiff.ac.uk](mailto:williamsb39@cardiff.ac.uk)  School of Earth and Environmental Sciences, Cardiff University, Cardiff, UK.  
Editorial handling: Chris Fergusson

 Supplemental data for this article is available online at <https://doi.org/10.1080/08120099.2022.2153384>

© 2023 The Author(s). Published by Informa UK Limited, trading as Taylor & Francis Group.  
This is an Open Access article distributed under the terms of the Creative Commons Attribution License (<http://creativecommons.org/licenses/by/4.0/>), which permits unrestricted use, distribution, and reproduction in any medium, provided the original work is properly cited.

timings of deformation and mineralisation have been determined using small-scale structures and past studies have also shown the importance of these small-scale structures in elucidating the structural controls on ore bodies at a larger scale (Bell *et al.*, 1988; Davis, 2004; Perkins, 1984; Swager, 1985). This study was initiated by the recognition of previously undescribed foliation boudinage structures observed at the core scale, proximal to the high-grade Cu ore bodies.

Foliation boudinage structures are vein-like boudin structures that form in highly anisotropic and homogeneous rocks during layer parallel extension and layer normal shortening of fractures (Platt & Vissers, 1980). Foliation boudinage structures are found within well foliated or finely laminated rocks where they form most commonly under greenschist and amphibolite facies conditions (Arslan *et al.*, 2008). Fracture dilation leads to an open central void that provides space for mineral precipitation. Aerden (1991) identified these structures to be a controlling feature of the Rosebery Pb–Zn deposit in Tasmania, where multiple foliation boudinage structures exist with dimensions of 100's of metres.

This study aims to highlight the presence of drill core-scale foliation boudinage structures at Mount Isa and their potential importance for Cu mineralisation by answering the following questions:

- What is the location, geometry, and timing of foliation boudinage structures?
- Is there any relationship between the foliation boudinage structures and Cu grades at Mount Isa?

## Background

### Regional geology

Mount Isa is located within the late Paleo- to early Mesoproterozoic Mount Isa Inlier (Figure 1). The Mount Isa Inlier can be subdivided into broad tectonic divisions as the Western Fold Belt, the Kalkadoon-Leichhardt Belt and the Eastern Fold Belt (Blake, 1987; Day *et al.*, 1983). The Mount Isa mine lies within the Leichhardt River Fault Trough of the Western Fold Belt. The Western Fold Belt is composed of a succession of volcanic and sedimentary rocks and is separated from the generally higher metamorphic grade and more deformed Eastern Fold Belt by the Kalkadoon-Leichhardt Belt (O'Dea, Lister, Betts, *et al.*, 1997; O'Dea, Lister, Maccready, *et al.*, 1997). The central Kalkadoon-Leichhardt Belt exposes crystalline basement rocks deformed and metamorphosed during the 1900–1870 Ma Barramundi Orogeny (O'Dea, Lister, Maccready, *et al.*, 1997; Page & Williams, 1988).

The post-basement stratigraphy of the Mount Isa Inlier is characterised by periods of intracontinental rifting and is commonly separated into the Eastern and Western successions (Blake, 1987; Blake & Stewart, 1992). The Western Succession broadly occurs in the Western and Kalkadoon-Leichhardt fold belts. The regional stratigraphy of the Western Succession constitutes basement metamorphics overlain by three stacked “superbasins”; the Leichhardt (1800–1750 Ma), Calvert (1735–1690 Ma) and Isa (1670–1575 Ma) superbasins (Jackson *et al.*, 2000; Page *et al.*, 2000; Scott *et al.*, 2000; Southgate *et al.*, 2000). The three superbasins did not experience significant large strain

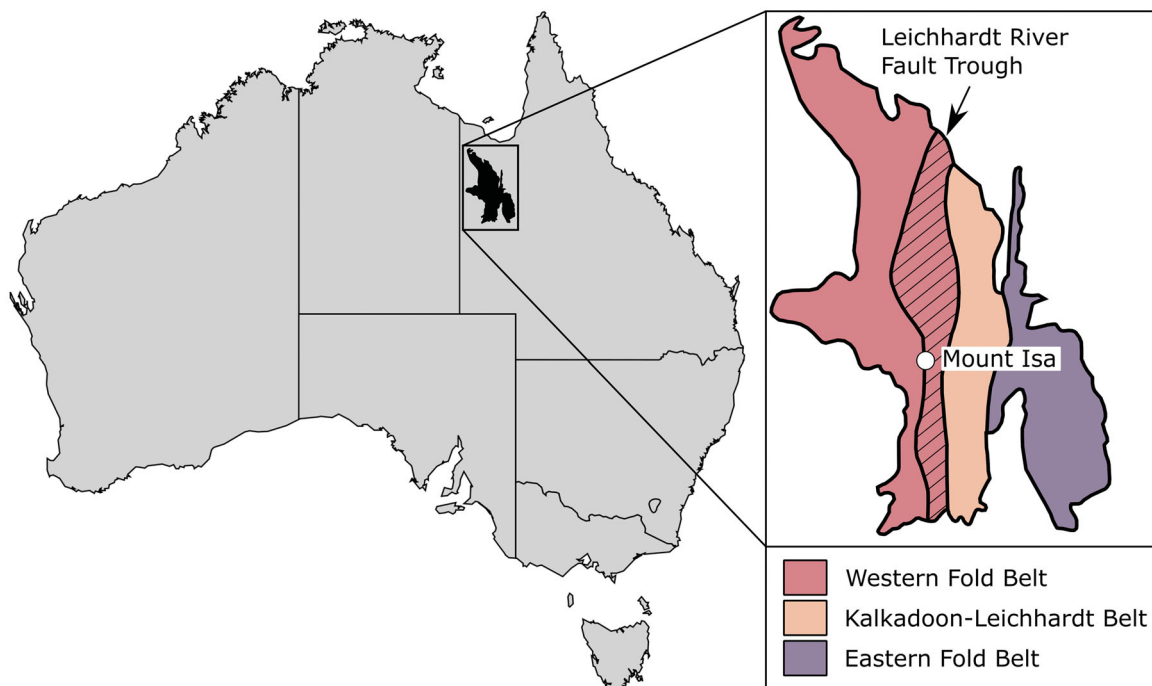
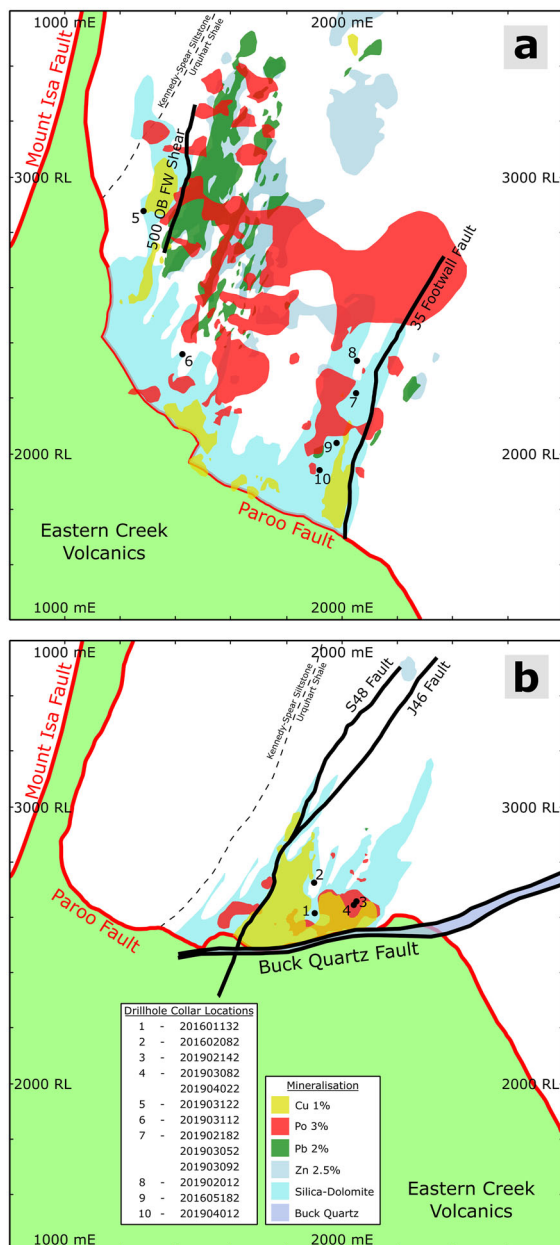


Figure 1. The location of Mount Isa and the main tectonic divisions of the Mount Isa Inlier of northwest Queensland, Australia, after Blake and Stewart (1992) and Davis (2004).



**Figure 2.** East–west cross-sections showing the relative positions of the Cu and Pb–Zn orebodies, pyrrhotite (Po) and silica-dolomite halos, and buck quartz at Mount Isa. Collar locations for drill holes analysed in this study are displayed as points and correspond to their relative positions in relation to the mineralisation (see Supplemental data, Table S1 for drill hole co-ordinates, downhole lengths, and orientations). (a) Cross-section in the north of the mine at 7000 mN. (b) Cross-section in the south of the mine at 4350 mN.

regional contraction prior to the onset of the Isan Orogeny (1610–ca 1500 Ma; O’Dea, Lister, Maccreeady, *et al.*, 1997).

The Leichhardt Superbasin comprises deep marine sediments of the 1790 ± 9 Ma Bottletree Formation (Page, 1983; Page & Sun, 1998) to later fluvial and shallow marine deposits of the 1773 ± 16 Ma Mount Guide Quartzite (Neumann *et al.*, 2006). The early Leichhardt sediments are succeeded by vast iron-rich continental flood basalts of the ca 1780 Ma Eastern Creek Volcanics, including the 1779 ± 4 Ma Lena Quartzite (Neumann *et al.*, 2006). The

overlying Myally Subgroup (1773 ± 2 Ma Bortala Formation and 1768 ± 8 Ma Whitworth Quartzite; Neumann *et al.*, 2006) consists of clastic sedimentary successions, largely controlled by extensional faulting (Betts *et al.*, 2006; O’Dea, Lister, Betts, *et al.*, 1997) and are overlain by shallow marine quartzites and carbonates of the 1763 ± 8 Ma Quilalar Formation (Betts *et al.*, 2006; Jackson *et al.*, 2000; Neumann *et al.*, 2006).

The Calvert Superbasin is largely composed of clastic fluvial and shallow-marine sediments, with interbedded bimodal volcanic rocks deposited in a half graben during northwest–southeast extension (Betts *et al.*, 1998, 1999; O’Dea, Lister, Betts, *et al.*, 1997). The 1762 ± 18 Ma Bigie Formation (Neumann *et al.*, 2006) unconformably and para-conformably overlies the Quilalar Formation and Myally Subgroup (Betts *et al.*, 1999) and is overlain by the 1709 ± 3 Ma Fiery Creek Volcanics (Page & Sweet, 1998) and Surprise Creek Formation.

Emplacement of the 1670 ± 3 Ma Sybella Granite (Neumann *et al.*, 2006) marks the boundary between the Calvert Superbasin and overlying Isa Superbasin, the latter being made up of the Gun, Loretta, River, Term, Lawn, Wide and Doom supersequences (Domagala *et al.*, 2000; Page *et al.*, 2000). In the Mount Isa region, the basal Gun and Loretta supersequences are dominated by carbonaceous shale, stromatolitic dolostone, and turbiditic sandstone and siltstone of the Mount Isa Group (Figure 3; Domagala *et al.*, 2000; Page *et al.*, 2000; Southgate *et al.*, 2000). The lithostratigraphy of the Mount Isa Group includes the 1668 ± 8 Ma Moondarra Siltstone (Southgate *et al.*, 2000), 1663 ± 3 Ma Breakaway Shale (Page *et al.*, 2000; Southgate *et al.*, 2000), Native Bee Siltstone, 1652 ± 7 Ma Urquhart Shale (Page *et al.*, 2000; Page & Sweet, 1998), Spear Siltstone, 1648 ± 3 Ma Kennedy Siltstone (Page *et al.*, 2000), and 1648 ± 3 Ma Magazine Shale (Page *et al.*, 2000).

### Deformation

Multiphase deformation during the Isan Orogeny is recorded in the western Mount Isa Inlier as a minimum of four deformation events (D1–D4a; Figure 4).

The 1610 ± 13 Ma (Page & Bell, 1986) D1 event was initially interpreted as a large-scale north to south directed thrust complex, producing local east–west oriented faults and an S1 axial planar cleavage (Bell, 1983, 1991; Bell *et al.*, 1988; Bell & Hickey, 1998; Blake, 1987; Davis, 2004; Page & Bell, 1986; Perkins, 1984; Perkins *et al.*, 1999; Swager, 1985; Wilde, 2011; Winsor, 1986). However, O’Dea, Lister, Betts, *et al.* (1997), O’Dea, Lister, Maccreeady, *et al.* (1997) and O’Dea and Lister (1995) dismissed the thrust duplex theory and have instead shown D1 produces east–west oriented reverse faults as a result of north–south shortening of previous syn-rift normal faults.

D2 involved east–west shortening, creating macroscopic north–south-striking upright folds with shallowly plunging regional anticlines and synclines (Bell, 1983; Bell *et al.*,

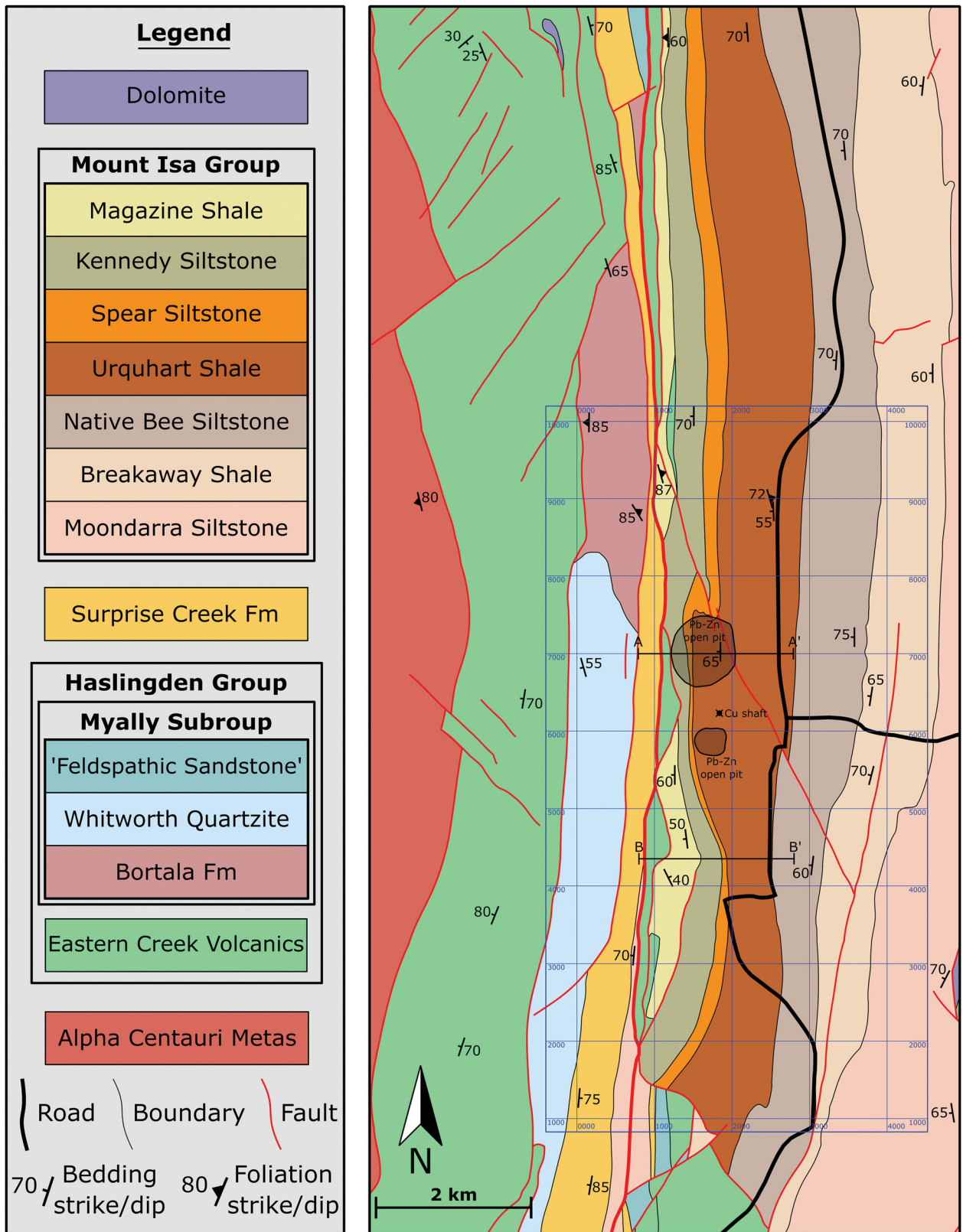
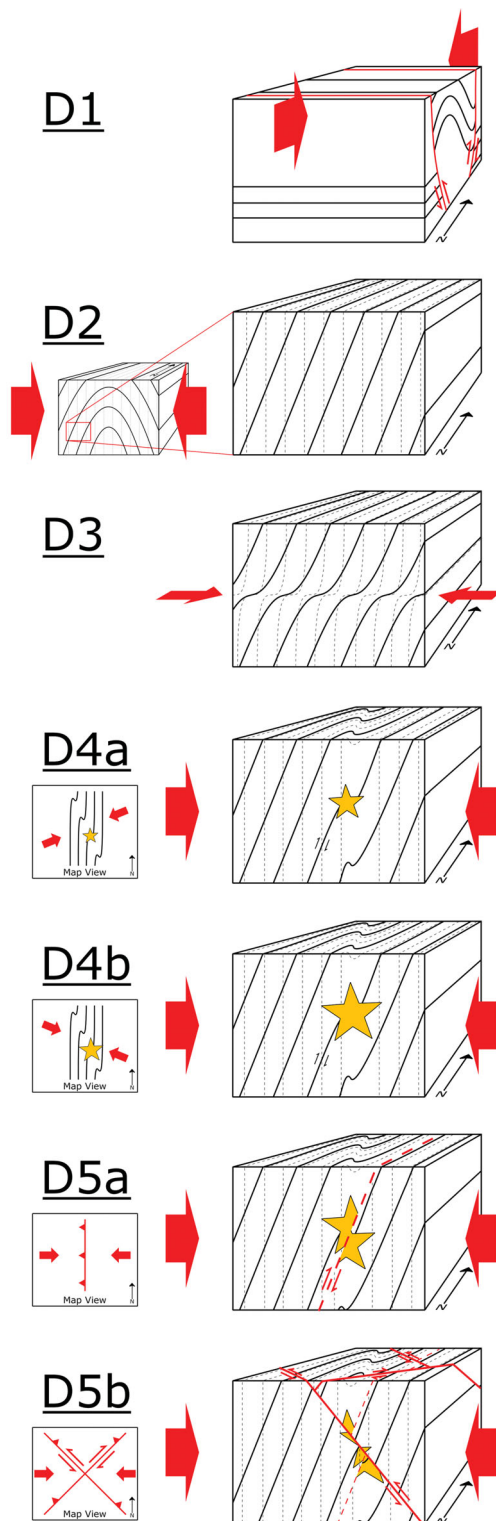


Figure 3. A geological map of the Mount Isa area with mine workings and local mine grid. After Spatial and Graphic Services, Statewide Operations, Department of Natural Resources (2020).



**Figure 4.** Summary of deformation events at Mount Isa based on previous deformation schemes (Bell *et al.*, 1988; Davis, 2004; Miller, 2007; O’Dea, Lister, Betts, *et al.*, 1997; O’Dea, Lister, Maccready, *et al.*, 1997; O’Dea & Lister, 1995; Perkins, 1984; Swager, 1985; Wilde, 2011). **D1**, localised reverse reactivation of normal faults as a result of north–south shortening; **D2**, east–west shortening; **D3**, top to the east shear, weakly developed at Mount Isa Mine; **D4a**, east–north–east–west–southwest shortening and mineralisation at Mount Isa; **D4b**, west–northwest–east–southeast shortening and mineralisation at Mount Isa; **D5a**, top to the east transport direction on west-dipping reverse faults; **D5b**, conjugate sinistral-reverse and dextral-reverse faults with top to the east or west transport directions consistent with continued east–west shortening.

1988; Bell & Hickey, 1998; Blake, 1987; Davis, 2004; Page & Bell, 1986; Perkins, 1984; Perkins *et al.*, 1999; Swager, 1985; Wilde, 2011). At Mount Isa Mine, a subvertical S2 axial planar foliation is generally bedding parallel within the Mount Isa Group (Swager, 1985; Wilde, 2011). Dolomite filled D2 extension veins formed at high angles to bedding and are truncated against bedding planes and contain fibres that are sub-parallel to S2 (Swager, 1985; Wilde, 2011). Early dating of D2 in the Western Fold Belt yielded ages of  $1532 \pm 7$  Ma (Connors & Page, 1995), but more recent studies have produced ages of *ca* 1575 Ma which are consistent with D2 ages from the Eastern Fold Belt (Duncan *et al.*, 2006). Peak metamorphism is recorded during D2 prograde metamorphism up to amphibolite facies.

D3 of Davis (2004; D2.5 of Bell & Hickey, 1998) is observed as sub-horizontal axial planes with reactivation and intensification of the existing S2 fabric by top to the east shear and rotation of S2 into shallower orientations (Bell & Hickey, 1998). This event is generally weak and spatially localised, being poorly developed at Mount Isa Mine (Bell & Hickey, 1998; Perkins, 1997).

D4a (D4 of Davis, 2004 and Wilde, 2011 and previously D3) locally formed north–northwest–south–southeast-striking fold zones with sub-vertical axial planes, rotating to a northwest strike in the north of the mine. Deformation is typically confined to 10–20 m wide fold zones in the Urquhart Shale, which are locally as much as 100 m wide. The Mount Isa Fold found at the north end of the mine is the largest of these F4 fold zones (Davis, 2004). Most folds in the mine belong to this D4a event, which is dated to  $1510 \pm 13$  Ma (Page & Bell, 1986). A S4 fabric sub-parallel to S2 is observed as a slaty cleavage in dolomitic shale and as a crenulation cleavage in black shale lithologies.

Miller (2007) documented D5a reverse faults and D5b conjugate reverse faults (his D4a and D4b) that overprint the Cu orebodies, as a result of continued east–west shortening. These D5a faults are described as typically steeply west-dipping structures that parallel the Mount Isa Fault Zone (Figure 3), with most D5a faults showing slip along bedding with a top to the east transport direction (Miller, 2007). The Buck Quartz Fault (Figure 2) is an example of a shallowly dipping D5a fault (Miller, 2007), which intersects the Paroo Fault beneath the Mount Isa deposit. The D5a faults are overprinted by later conjugate northwest-trending sinistral-reverse and northeast-trending dextral-reverse strike-slip faults (Miller, 2007). The D5b faults have top to the east and top to the west hangingwall transport directions for the northeast-trending and northwest-trending faults, respectively, consistent with east–west shortening (Miller, 2007). The S48 fault (Figure 2) is an example of a northeast-trending D5b fault that overprints the Cu mineralisation.

### Deposit geology

The Cu orebodies are hosted within the Urquhart Shale unit of the Mount Isa Group and are situated on the

steeply ( $\sim 65^\circ$ ) west-dipping limb of a regional D2 anticline (Figure 2; Bell *et al.*, 1988). The Urquhart Shale comprises a sequence of finely laminated interbedded dolomitic shales, siltstones, and mudstones that produces a strong structural anisotropy (Davis, 2004; Neudert, 1983).

The north–south orientated Mount Isa Fault (Figure 3) juxtaposes amphibolite facies rocks to the west with greenschist facies to the east (Bell, 1991; Bell & Hickey, 1998; Davis, 2004; Perkins *et al.*, 1999; Rubenach, 1992). East of the Mount Isa Fault in the mine vicinity, Eastern Creek Volcanics are separated from the overlying Urquhart Shale by the sigmoidal-shaped Paroo Fault (Davis, 2004; Long, 2010). To the west and east of the deposit the Paroo Fault is sub-vertical, but has an undulating geometry beneath the Cu orebodies where it is termed the basement contact (Bell *et al.*, 1988; Davis, 2004). The largest Cu orebodies (1100, 1900, 3000 and 3500) are adjacent to the Paroo Fault and smaller (200, 500 and 650) orebodies are located at a greater distance (Davis, 2004). The Cu orebodies were interpreted to be associated with north–northwest-plunging F4 fold hinges (Bell *et al.*, 1988; Davis, 2004; Perkins, 1984) and recent investigations have shown the potential presence of a deep feeder structure relating to the north–northwest-trending Bernborough Fault (Andrew, 2020). A south to north directed hydrothermal fluid pathway has previously been determined through mineralogical and geochemical alteration patterns (Andrew, 2020; Waring, 1990).

The Cu orebodies occur as large bodies (10's to 100's m) of chalcopyrite-rich breccia that are hosted within silica-dolomite alteration halos (Perkins, 1984). Variably brecciated silica-dolomite produces four main rock types that reflect silicification ('siliceous shale' and 'brecciated and fractured siliceous shale') and dolomitisation ('recrystallised shale' and 'irregularly brecciated and recrystallised shale') of the host rock (Clark, 1968; Knights, 1976; Mathias & Clark, 1975; Miller, 2007; Perkins, 1984). Dolomite overprints quartz, with both quartz and dolomite dissolution interpreted to have occurred during chalcopyrite mineralisation (Wilde, 2011; Wilde *et al.*, 2006). Fine-grained pyrite, silica-dolomite, calcite, quartz, and coarse-grained pyrite all pre-date chalcopyrite (Cave *et al.*, 2020; Gulson *et al.*, 1983; Perkins, 1984). Perkins (1984) and Swager (1985) showed silicification and dolomitisation were coincident with D4a. Previous studies have shown that the brecciation post-dates the S4 cleavages, with S4 cleavages observed within rotated shale clasts (Bell *et al.*, 1988; Miller, 2007; Perkins, 1984).

Pyrrhotite is most prevalent in the zone between the Pb–Zn orebodies and Cu mineralisation (Perkins, 1984), with only minor chalcopyrite occurring in pyrrhotite-dominated lithologies (Cave *et al.*, 2020). Chalcopyrite is commonly considered to be coeval to pyrrhotite (Cave *et al.*, 2020) and forms replacive growths across all generations of veins and microstructures (Miller, 2007; Perkins, 1984). Recent studies have suggested an epigenetic origin

for both the Pb–Zn and Cu ore bodies (Cave *et al.*, 2020), with the timing of Cu mineralisation as post-peak metamorphism during the D4a shortening event (Perkins, 1984; Smith *et al.*, 1978; Swager, 1985; Wilde, 2011). Conversely, Miller (2007) proposed that the Cu ore bodies developed during a post-D4a, pre-D5a sinistral-reverse strike-slip event, with a stress field distinct from D4a, which we have termed D4b.

### Foliation boudinage structures

Drill cores from Mount Isa contain foliation boudinage structures with similar mineralogical relationships to those documented in the Mount Isa Cu deposit, although these foliation boudinage structures have not been recognised previously. Analogue modelling by Mandal and Karmakar (1989) and computer modelling by Arslan *et al.* (2008, 2012) demonstrated how foliation boudinage structures develop in highly anisotropic and homogeneous materials. Foliation boudinage structures form by the ductile deformation of foliation or layering around a brittle fracture (Arslan *et al.*, 2008) and have been identified in rocks and glacier ice that exhibit significant anisotropy (Arslan *et al.*, 2008; Hambrey & Milnes, 1975; Platt & Vissers, 1980; Wiest *et al.*, 2020). Deformation of fractures during layer-normal shortening may lead to the opening of voids that accommodate infill (Arslan *et al.*, 2008). The characteristic bending or necking of the layering into the fracture defines the neck of the foliation boudinage structure (Arslan *et al.*, 2008) and is most readily identified in cross-section normal to the foliation boudin long axis (Y-direction; Figure 5). Arslan *et al.* (2008) and Goscombe *et al.* (2004) showed that the long axis of boudins and foliation boudinage structures represents the intermediate principal strain axis.

Foliation boudins could be considered fractal structures identifiable on multiple scales from millimetres to at least 10's of metres (Arslan *et al.*, 2008). The largest structures contain 10's to 100's of cubic metres of infill and can form fishmouth structures as the central void recloses (Aerden, 1991; Arslan *et al.*, 2008; Goscombe *et al.*, 2004; Swanson, 1992). Infill is generally massive quartz, calcite or other common vein-forming minerals (Arslan *et al.*, 2008).

Foliation boudinage structures can be separated into two broad types: symmetrical and asymmetrical (Figure 6; Hambrey & Milnes, 1975; Milnes, 1964). The symmetrical types form in coaxial flow around Mode I extension fractures and can produce infill in lozenge-shaped voids (Arslan *et al.*, 2008; Mandal & Karmakar, 1989; Platt & Vissers, 1980). Asymmetrical foliation boudinage structures can form under coaxial flow of oblique fractures or by non-coaxial flow of shear fractures where they display antithetic displacements (Arslan *et al.*, 2008; Mandal & Karmakar, 1989; Platt & Vissers, 1980). Asymmetric foliation boudinage structures can form as single fractures or as conjugate sets (Arslan *et al.*, 2012; Sawyer, 1983).

The presence of foliation boudinage structures with similar formation mechanisms but different geometries indicate a continuum of deformation with filling occurring at any stage of their formation (Arslan *et al.*, 2008). A lack of deformation within the void fill implies a protracted period of time between foliation boudin formation and a final stage of infill (Arslan *et al.*, 2008; Hambrey & Milnes, 1975; Platt & Vissers, 1980). Arslan *et al.* (2008) suggested that open fluid-filled voids could occur for a substantial period of time before mineral precipitation providing the fluid pressure is significantly high.

## Methods

Thirteen drill holes from the Mount Isa Copper Operations (MICO) and two from Resource Development (RD) were logged for structures of interest related to sulfide mineralisation. All drill holes examined in the study are from within the Mount Isa system. The MICO drill holes were drilled underground from a range of areas within the deposit but are generally close to or intersect high-grade Cu mineralisation. The two RD drill holes were drilled from the surface into the periphery of the Mount Isa system. The drill cores were chosen based on availability during core logging and represent various locations across the ore body (Figure 2; Supplemental data, Table S1).

Structural measurements were collected from both the MICO and RD drill cores, although only the RD drill holes (T667ED1 and T190ED1) are oriented. Consequently, only structural measurements from the RD drill holes have been used in this study. The long axes of foliation boudinage structures (Y-direction; Figure 5) were defined by the pinching of the layering into the neck regions. Using the fold hinge method of Blenkinsop *et al.* (2015), orientations of the foliation boudinage structures were measured as linear

fold hinges where the neck regions were observed on opposite sides of the drill core. Structural measurements were collected using an EZY-Logger goniometer and the orientations of foliation boudinage structures were determined using drill core  $\alpha$  and  $\beta$  angles together with the drill hole survey data (Vearncombe & Vearncombe, 1998).

Assays and MICO/RD logs were available. The lithologies logged in the drill holes differentiate progressively deformed and altered lithologies and are termed 'Shale', 'Pyritic Shale (5–20% pyrite)', 'Pyritic Shale (>20% pyrite)', 'Recrystallised Shale', 'Irregularly Brecciated and Recrystallised Shale', 'Siliceous Shale', 'Brecciated and Fractured Siliceous Shale', 'Carbonaceous Mylonite', 'Buck Quartz' and 'Greenschist'. The sulfide infills of the drill core-scale foliation boudinage structures were recorded and their positions logged as downhole distances.

Drill-core samples containing foliation boudinage structures were collected for detailed analysis. Cross-sections were cut through the structures; polished thin sections were made for petrographic analysis and phase maps were collected using a scanning electron microscope (SEM).

## Results

### Petrography

In the host rock surrounding the ore bodies, fine-grained pyrite replaces shale selectively along layers (Figure 7a and Figure 8). Small veinlets of quartz occur normal or oblique to layering; their timing is generally early, forming after the fine-grained pyrite and before the coarse-grained pyrite (Figure 7a, b). Coarse-grained pyrite comprises euhedral to subhedral crystals ranging in size from 500  $\mu\text{m}$  to mm, occurring as single porphyroblasts or in trains at contacts between particular shale beds (Figure 7a). The coarse-

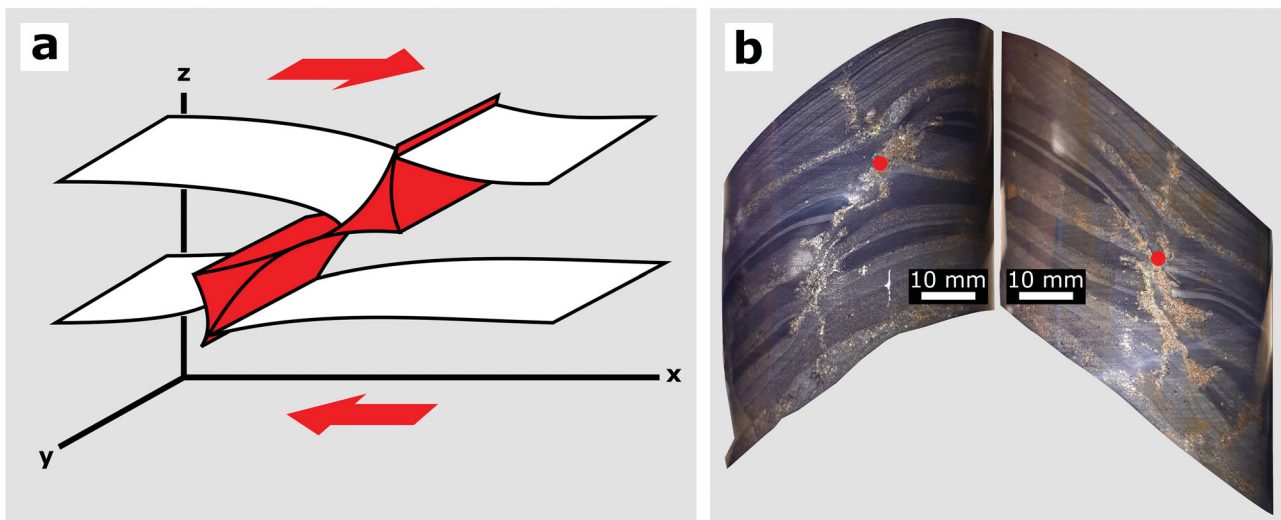


**Figure 5.** Measuring orientations of foliation boudinage structures in drill core. (a) Reference axes of foliation boudinage structures showing the pinching of layering into the neck region. The long axis of the structure is in the Y-direction and cross-section in the XZ-plane. (b) A foliation boudinage structure from drill hole '201903092' as seen on opposite sides of the drill core. The sample was located at a downhole distance of 32.1 m. Diameter of drill core is ~50 mm. The neck lineation is defined by the red dots.



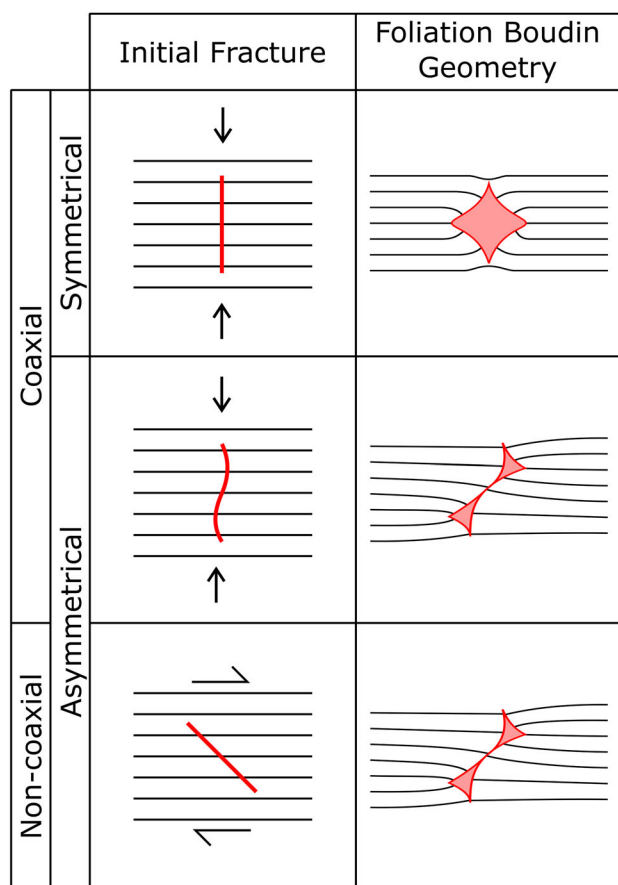


Figure 6. The formation mechanisms of common symmetrical and asymmetrical foliation boudinage structures by coaxial and non-coaxial deformation as seen in cross-sectional view based on Arslan *et al.* (2008, 2012), Hambrey and Milnes (1975), Mandal and Karmakar (1989) and Platt and Vissers (1980). Approximate layer normal shortening (arrows) and layer parallel extension of the fracture (red line) allows the formation of the foliation boudinage structures.

grained pyrite is commonly zoned (Figure 7c) and is associated with later arsenopyrite growth rims (Cave *et al.*, 2020). Dolomite replaces shale layering, occurring throughout layers or as lenses (Figures 7d, 9c and 10a, b, d, f). Brecciation occurs with silica-dolomite infilling between shale clasts with some alteration of the shale (Figure 7b). Pyrrhotite occurs as infill in silica-dolomite breccia and replacement in dolomitic layers (Figure 7d). Chalcopyrite occurs as veins and replacement and varies in samples from pre-, syn- to post-pyrrhotite (Figure 7e, f).

Asymmetrical foliation boudinage structures are the most common type observed in Mount Isa drill core (Figure 9). Foliation boudinage structures and polished sections of cross-sections through the structures are shown in Figure 10. Dolomite replaces shale layers and forms lenses adjacent to some foliation boudin samples (Figures 9c and 10b, d). Regular boudins are observed in these dolomitic layers close to the foliation boudinage structures where they show an equivalent petrography, with silica-dolomite rims and sulfide infills (Figure 10d, f). Coarse-grained pyrite with quartz strain shadows are observed in close proximity to the foliation boudinage structures in some samples.

Quartz veins normal to the layering and veinlets oblique to the layering are cross-cut and deformed by the foliation boudinage structures (Figure 10a–c, g).

All foliation boudinage structures analysed in this study are completely filled by a combination of quartz, dolomite, pyrrhotite and minor chalcopyrite. Quartz infilling around the edges of the interior of the foliation boudinage structures creates a rim of quartz growth into the structures (Figures 9 and 10). Later coarse-grained dolomite is the dominant non-sulfide infill in the foliation boudinage structures and occurs within the quartz rim. The dolomite infill and quartz rim both show deformation in the form of deformation twins and undulose extinction, respectively. In places, the silica-dolomite also alters the wall rock and appears to propagate from the foliation boudinage structure (Figure 10b).

Pyrrhotite is the most abundant mineral found within the foliation boudinage structures. The pyrrhotite shows an infill texture around dolomite and quartz grains and is observed replacing dolomite (Figure 10e). Chalcopyrite is observed in only a few foliation boudinage structures on the drill core scale, where it is intergrown with pyrrhotite (Figure 9b). Within one foliation boudinage structure, chalcopyrite cross-cuts the pyrrhotite as a vein style or late infill mineralisation, giving a post-pyrrhotite timing (Figure 10g).

#### Foliation boudinage structure orientations

The long axes of drill core-scale foliation boudinage structures form a predominant north–south lineation with gentle to moderate plunges (Figure 11). Bedding orientations change slightly from a west-southwest to a west-northwest dip direction with increasing depth down RD drill hole T667ED1 (Figure 11) and are representative of the dominant orientations in the mine. The long axis orientations of foliation boudinage structures also vary with depth, changing from north-northwest–south-southeast to north-northeast–south-southwest trends at greater depths (Figure 11). The foliation boudinage structures always lie on or close to the local bedding (Supplemental data, Figure S1). A Terzaghi correction (Terzaghi, 1965; Wallis *et al.*, 2020) was performed on the bedding measurements but made no discernible difference as the drilling orientation is at a high angle to bedding.

#### Distribution of foliation boudinage structures by rock type

A total of 255 foliation boudinage structures were observed in the MICO and RD drill core and have been normalised by the total length of the lithologies in which they were located (Figure 12). By far the most common rock type for foliation boudinage structures is the relatively undeformed Urquhart Shale (Supplemental data, Table S2), and when normalised, also has the greatest number of foliation boudinage structures per metre (Figure 12). No foliation boudinage structures were identified in the 'pyritic shale (>20% pyrite)', 'carbonaceous mylonite', 'buck quartz' or 'greenschist' lithologies.

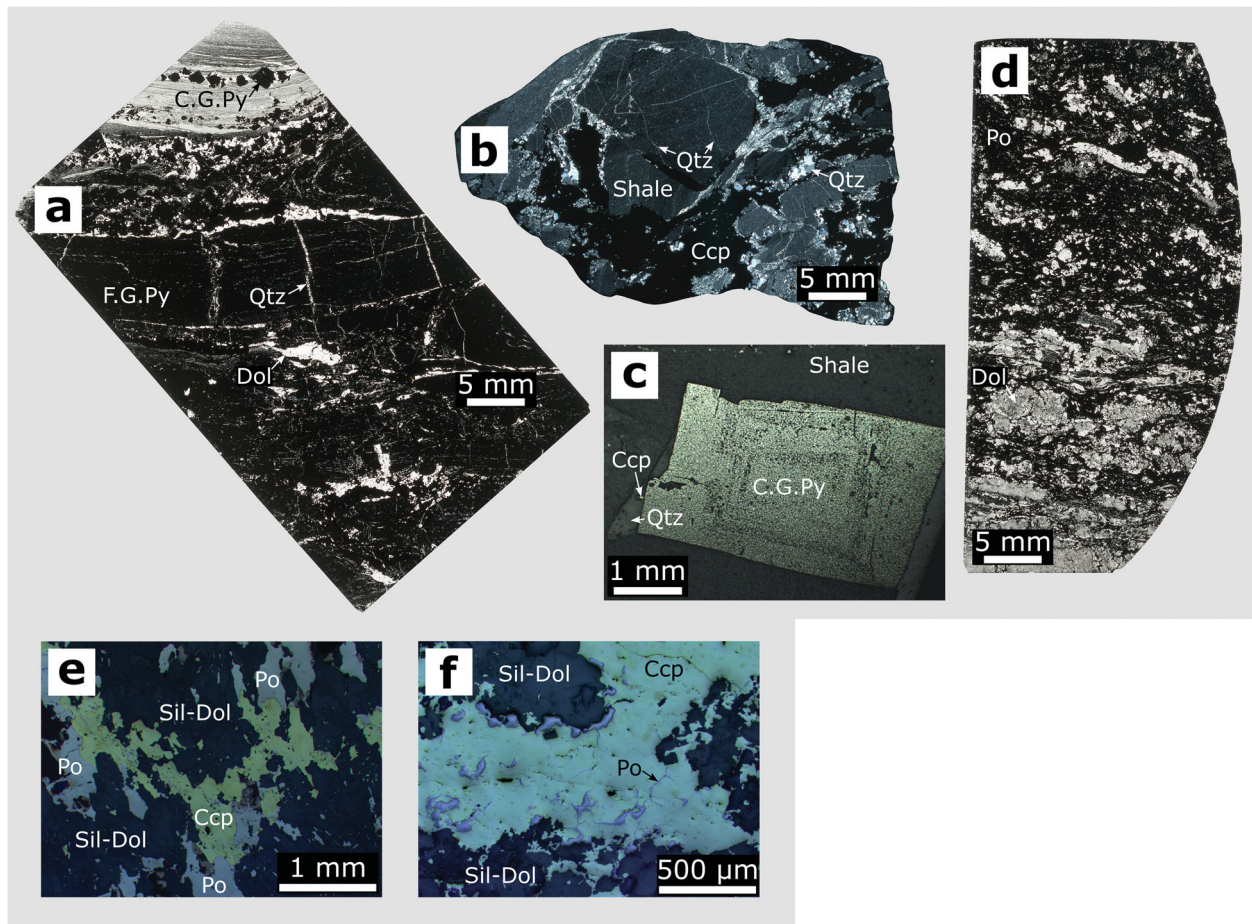


**Figure 7.** Polished sections from underground samples and drill core in the Mount Isa system. (a) Fine-grained pyrite selectively replacing shale layers, with later quartz veinlets. Coarse-grained pyrite restricted to contacts between select shale layers. Sample BW304B, Drill hole № '201904012', 36.65 m (PPL). (b) Silica-dolomite and chalcopyrite breccia associated with the main Cu mineralisation event. Shale clasts show small pre-brecciation quartz veinlets. Sample BW308, collected from underground proximal to Cu orebodies (XPL). (c) Zoned coarse-grained pyrite with quartz and chalcopyrite in strain shadow. Sample 'F', Drill hole № '201903092', 32.1 m (RL). (d) Coarse-grained dolomite alteration of shale layering that is subsequently replaced by pyrrhotite. Sample BW205, Drill hole № '201903092', 152.8 m (PPL). (e) Early-pyrrhotite and later chalcopyrite in silica-dolomite. Sample BW201B, Drill hole № '201904012', 175.5 m (RL). (f) Early chalcopyrite with later pyrrhotite in silica-dolomite. Sample BW402, Drill hole № '201903092', 168 m (RL). Key: Ccp, chalcopyrite; C.G.Py, coarse-grained pyrite; Dol, dolomite; Po, Pyrrhotite; Qtz, quartz; Shale, unaltered shale; Sil-Dol, silica-dolomite; Sul, multiple sulfides; PPL, plane-polarised light; XPL, cross-polarised light; RL, reflected light.

Mineral	Pre-FBS	FBS Infill
Pyrite (F.G)	■	
Quartz	■	■
Pyrite (C.G)	■	
Arsenopyrite	■	
Dolomitisation	■	
Silicification	■	
Dolomite		■
Pyrrhotite		■
Chalcopyrite		■
Deformation stage	Pre-D4a	D4a (early) D4a N-plunge FBS D4b S-plunge FBS

**Figure 8.** Paragenetic chart of the main mineralisation associated with foliation boudinage structures at Mount Isa.

### Distribution of ore-grade Cu by rock type

Lengths of drill-core intervals with ore-grade Cu (>3 wt% Cu) are normalised to the total lengths of each lithology and plotted against the logged drill-core lithologies (Figure 13; Supplemental data, Table S2). In the 47.7 m of drill core at greater than 3 wt% Cu, the most common rock type is the 'brecciated and fractured siliceous shale'. The ore-grade Cu is situated primarily in the brecciated and altered lithologies, with no Cu greater than 3 wt% in the 'pyritic shale (>20% pyrite)', 'carbonaceous mylonite', 'buck quartz' or 'greenschist'.

### Cu grade of foliation boudinage structures

Downhole Cu percentages and locations of foliation boudinage structures for three example drill holes are presented in Figure 14. Foliation boudinage structures are predominantly located in drill-hole intervals with the lowest

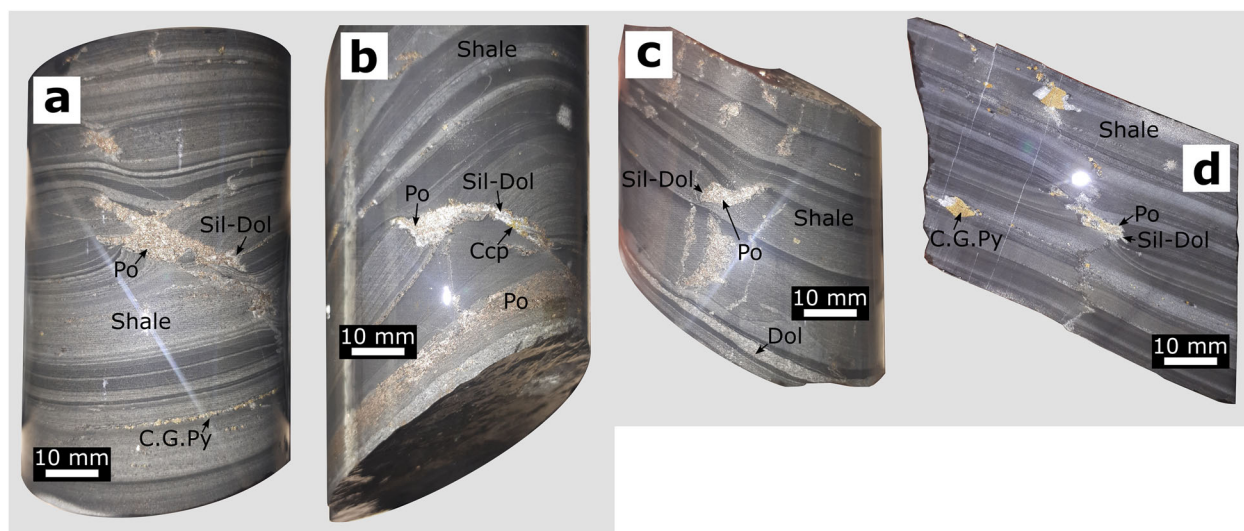


**Figure 9.** Photographs of asymmetrical foliation boudinage structures from Mount Isa drill core. (a) Pyrrhotite-filled foliation boudinage structure with silica-dolomite rim. Coarse-grained pyrite can be seen along one shale layer interface. Drill hole № '201903052', 23.5 m (all depths downhole). (b) Pyrrhotite and chalcopyrite-filled foliation boudinage structure with silica-dolomite rim. Pyrrhotite also replacing along a shale layer. Drill hole № '201902182', 16.1 m. (c) Pyrrhotite-filled foliation boudinage structure with silica-dolomite rim. Dolomite replacing shale layering. Drill hole № '201903092', 2.4 m. (d) Pyrrhotite-filled foliation boudinage structure with silica-dolomite rim. Coarse-grained pyrite has bedding parallel strain shadows and is cut by a bedding normal vein. Drill hole № 'T667ED1', 1202.2 m. Key: Ccp, chalcopyrite; C.G.Py, coarse-grained pyrite; Dol, dolomite; Po, Pyrrhotite; Qtz, quartz; Shale, unaltered shale; Sil-Dol, silica-dolomite; Sul, multiple sulfides.

Cu percentages and almost always below 3 wt% grade Cu (Supplemental data, Figure S2).

## Discussion

### Paragenesis

The petrographic observations in this study show that quartz forms an initial rim inside the foliation boudinage structures with a subsequent dolomite infill (Figures 9 and 10). This characteristic, seen in all the sampled foliation boudinage structures from Mount Isa, suggests that the infill mineralisation of the foliation boudinage structures was syn-silica-dolomite and the structures developed during this event. Within the Cu ore bodies, the silica-dolomite generally forms a breccia fill around shale clasts (Bell *et al.*, 1988; Cave *et al.*, 2020; Perkins, 1984) and is not conducive to the formation or preservation of the foliation boudinage structures as the breccia lacks the necessary anisotropy. No samples of foliation boudinage structures have yet been identified in brecciated shale clasts at Mount Isa. The foliation boudinage structures may have a pre- to syn-breccia timing, forming within the silica-dolomite halo, but distally to the breccia zone.

Pyrrhotite both replaced and infilled around the earlier silica-dolomite grains within the foliation boudinage structures (Figure 10), consistent with the post-silica-dolomite timing of most pyrrhotite at Mount Isa (Cave *et al.*, 2020; Perkins, 1984). Pyrrhotite is the most abundant sulfide mineral within the foliation boudinage structures and occurs within every sampled structure. Miller (2007) noted that the pyrrhotite has a strong correlation with the Cu, dolomite, and siliceous inner core and the data presented in this study broadly agrees with this relationship.

Only around 8% of the sampled drill core-scale foliation boudinage structures contain chalcopyrite. Where chalcopyrite is present, it occurs either coeval with the pyrrhotite or as vein-like mineralisation cross-cutting the pyrrhotite infill (Figure 10g). Pyrrhotite has been observed to be intimately associated with the chalcopyrite, and textural evidence shows both quartz and dolomite dissolution during chalcopyrite formation (Wilde *et al.*, 2006). Miller (2007) and Perkins (1984) describe strain free quartz associated with the chalcopyrite mineralisation. However, quartz and dolomite within the foliation boudinage structures have indications of strain.

### Foliation boudinage structure logging and scaling limitations

Foliation boudinage structures are predominantly located within the less deformed and altered lithologies (Figure 12) as a result of the shale layering or a layer parallel foliation providing the anisotropy and homogeneity of these rock types. Foliation boudinage structures could not form in rocks that lost their anisotropy during brecciation, deformation and alteration. The dolomitisation and silicification of the shale is generally considered to be an early alteration with subsequent brecciation associated with the silica-dolomite and Cu ore (Cave *et al.*, 2020; Perkins, 1984; Swager, 1985).

Perkins (1984) showed that dolomite porphyroblasts truncate and overgrow S2 cleavages, indicating a post-D2 age for this dolomitisation. Perkins (1984) also observed that the dolomite is both truncated by and overgrows the S4 cleavages and this has been used as evidence for a syn-

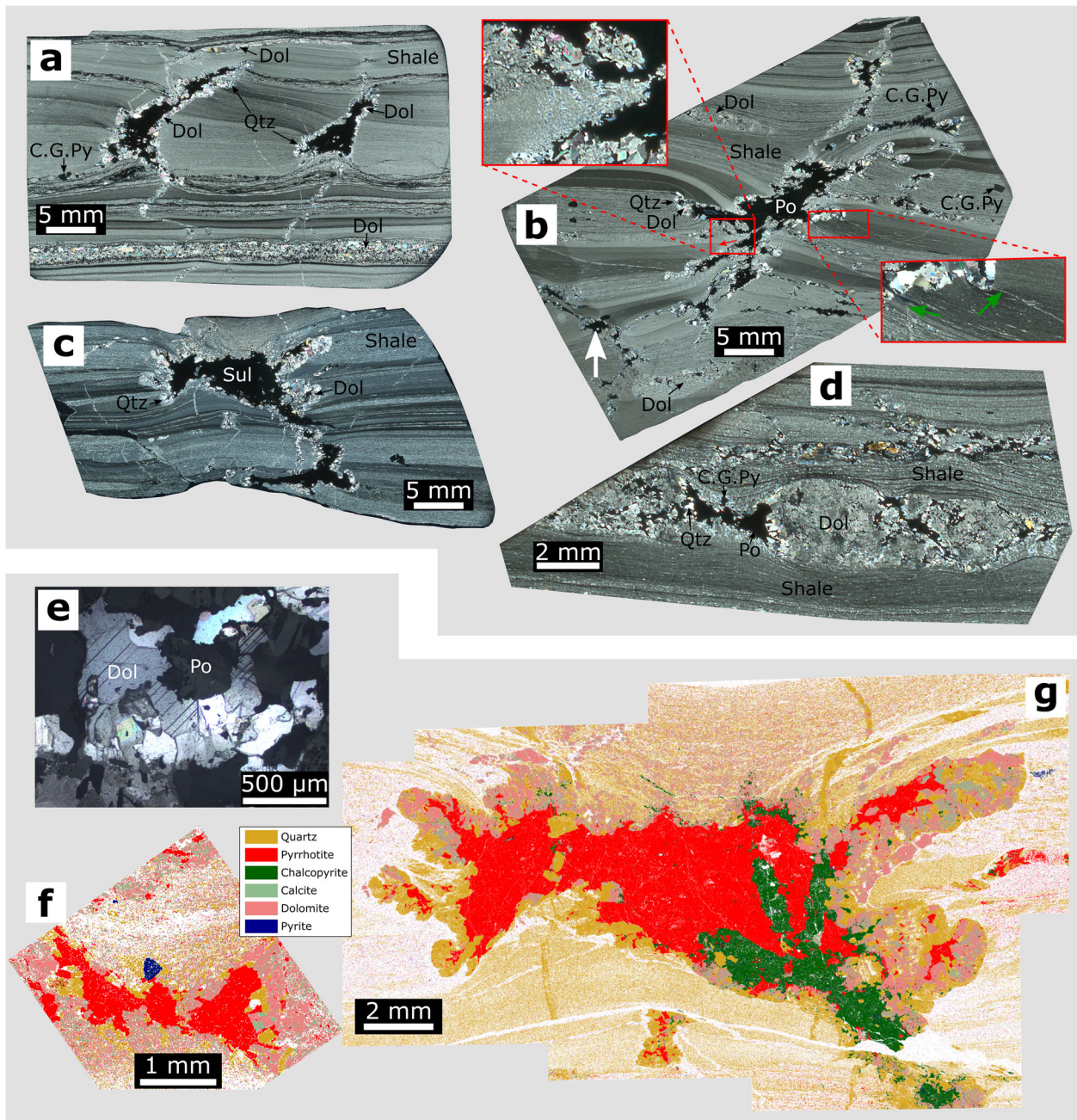


**Figure 10.** Polished sections and scanning electron microscope (SEM) phase maps of foliation boudinage structures from drill core in the Mount Isa system. (a) Pyrrhotite-filled foliation boudinage structures with silica-dolomite rims. Coarse-grained pyrite along a layer interface and dolomite replacing shale. Sample 'BW302', Drill hole № '201903092', 8.0 m (XPL). (b) Pyrrhotite-filled foliation boudinage structure with silica-dolomite rim. Coarse-grained pyrite throughout sample. A lens of dolomite replaces shale. Silica-dolomite alteration of the shale away from the foliation boudinage structure is represented by a red arrow. Pre-foliation boudinage veins are cross-cut and deformed by the foliation boudinage structure (green arrows). A smaller foliation boudinage structure indicating a conjugate set is seen at bottom left of polished thin section (white arrow). Sample 'E', Drill hole № '201903092', 32.1 m (XPL). (c) Pyrrhotite and chalcopyrite infilled foliation boudinage structure with silica-dolomite rim. Pre-foliation boudinage veins are cross-cut and deformed by the foliation boudinage structure. Sample 'BW303', Drill hole № '201904012', 159.3 m (XPL). (d) Pyrrhotite-filled boudin within a dolomite layer adjacent to a foliation boudinage structure. The competency difference between the shale and the dolomite enables the formation of boudins. A coarse-grained pyrite grain can be seen in the pinched neck of the boudin. Sample 'G', Drill hole № '201903092', 32.1 m (XPL). (e) Pyrrhotite replacing dolomite grain within the interior of a foliation boudinage structure. Sample 'BW205', Drill hole № '201903092', 152.8 m (XPL + RL). (f) Phase map of the boudin within the dolomite layer in (d), showing the pyrrhotite infill similar to the foliation boudinage structures (key in figure). Sample 'G', Drill hole № '201903092', 32.1 m. (g) Phase map of the interior of (c) showing the quartz and dolomite rim. The later pyrrhotite infills around and replaces earlier grains of dolomite. A later vein-like chalcopyrite mineralisation cuts through the pyrrhotite mass. Sample 'BW303', Drill hole № '201904012', 159.3 m. Key: Ccp, chalcopyrite; C.G.Py, coarse-grained pyrite; Dol, dolomite; Po, Pyrrhotite; Qtz, quartz; Shale, unaltered shale; Sil-Dol, silica-dolomite; Sul, multiple sulfides; PPL, plane-polarised light; XPL, cross-polarised light; RL, reflected light.

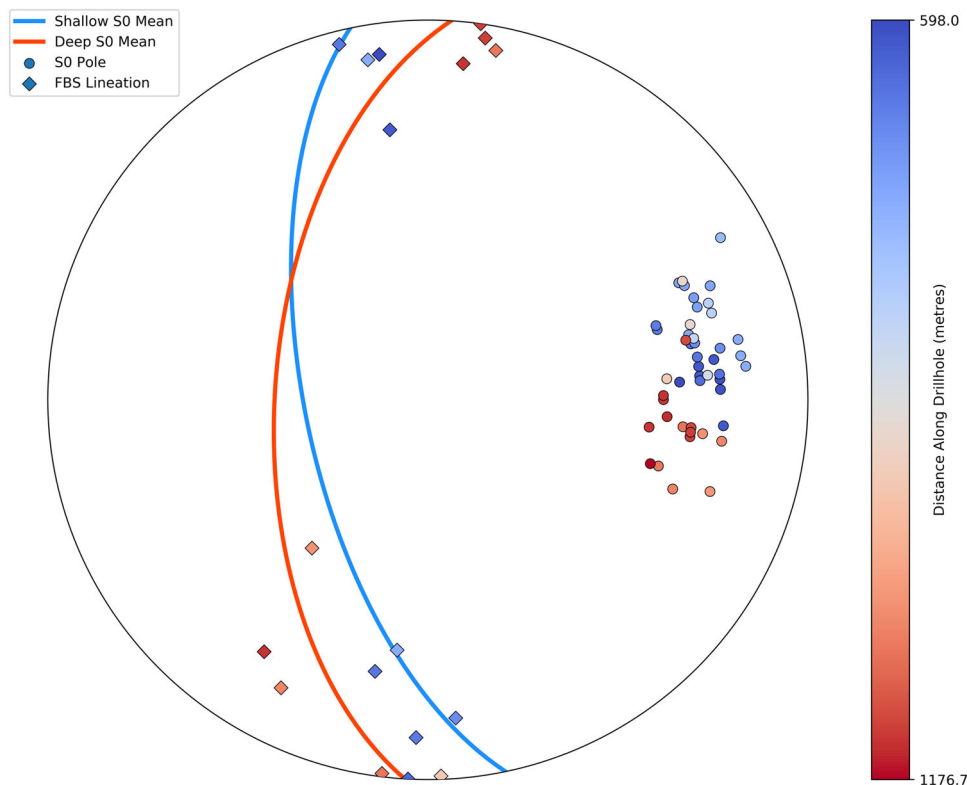


**Figure 11.** Lower hemisphere, equal area stereoplot of poles to bedding (circles) and foliation boudinage structures (diamonds) shaded by distance along drill hole T667ED1. Mean bedding planes are shown as great circles for shallow (blue) and deep (red) measurements that coincide with foliation boudin orientation changes with distance. Drill hole No. 'T667ED1', drill hole collar azimuth =  $087^\circ$  and inclination =  $-75^\circ$ .

D4a timing for dolomite porphyroblast growth (Miller, 2007). Foliation boudinage structures are generally absent in the dolomitised layers, possibly due to their heterogeneity and increased shear strength. Instead, regular boudins can be seen in these layers, owing to the development of a competency contrast between the ductile shale and more competent dolomite (Figure 10d, f). The foliation boudinage structures are interpreted to have formed coeval with and adjacent to the regular boudins, and both have a post-dolomitisation timing.

Silicification of the shale is considered to have a post-dolomitisation timing (Cave *et al.*, 2020; Perkins, 1984; Swager, 1985). Siliceous shales and brecciated siliceous shales generally form the inner core of the deposit, with most Cu mineralisation associated with these lithologies (Perkins, 1984). Relatively few foliation boudinage structures formed in the siliceous shale lithology (Figure 12). Where they are observed, they are interpreted to have a post-silicification timing as the foliation boudinage structures are not overprinted by the silicification process. The foliation boudinage structures located in the siliceous shale are commonly filled with chalcopyrite, reflecting the closer proximity to the high-grade Cu mineralisation.

The ore-grade Cu is in the more deformed and altered lithologies, close to or within the zone of brecciation as shown in Figure 13. A greater proportion of high-grade Cu in the more altered lithologies is expected as the silica-

dolomite alteration and brecciation are generally understood to lay the groundwork for the subsequent Cu mineralisation (Bell *et al.*, 1988; Cave *et al.*, 2020; Miller, 2007; Perkins, 1984; Swager, 1985). The shale lithology has by far the most foliation boudinage structures (Supplemental data, Table S2), but is not typically associated with high-grade Cu (e.g. Bell *et al.*, 1988; Cave *et al.*, 2020; Davis, 2004; Miller, 2007; Perkins, 1984; Swager, 1985; Swager *et al.*, 1987). Contrary to this general relationship, Figure 13 shows that there is some high-grade Cu in the shale lithology. This may be due to narrow chalcopyrite veins that intersect the shale.

Arslan *et al.* (2008) showed that foliation boudinage structures occur on scales similar to those found at Mount Isa and also on scales much larger than drill core. Aerden (1991) demonstrated the importance of these large-scale foliation boudinage structures on the control of ore bodies at the Rosebery deposit, Tasmania. The ore bodies at Rosebery occur in similar rock types and deformation styles to those at Mount Isa. Although they have not been identified during this study, large-scale foliation boudinage structures may exist and exert controls on the Cu ore bodies at Mount Isa. Davis (2004) showed that the Mount Isa Cu ore-bodies were steeply dipping with shallow to moderate plunges to the north and northwest, consistent with the orientations of the northwest-plunging small-scale foliation boudinage structures observed in this study. The drill holes

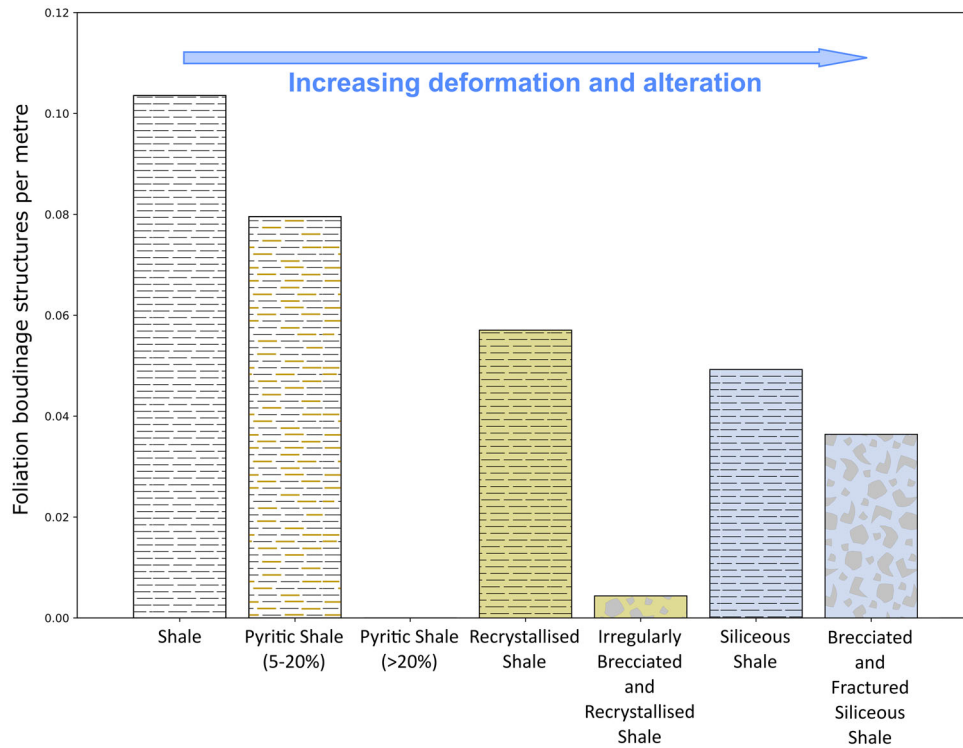


Figure 12. Normalised occurrences of foliation boudinage structures per lithology in the Mount Isa drill core. Foliation boudinage structures are identified most commonly in the less deformed lithologies.

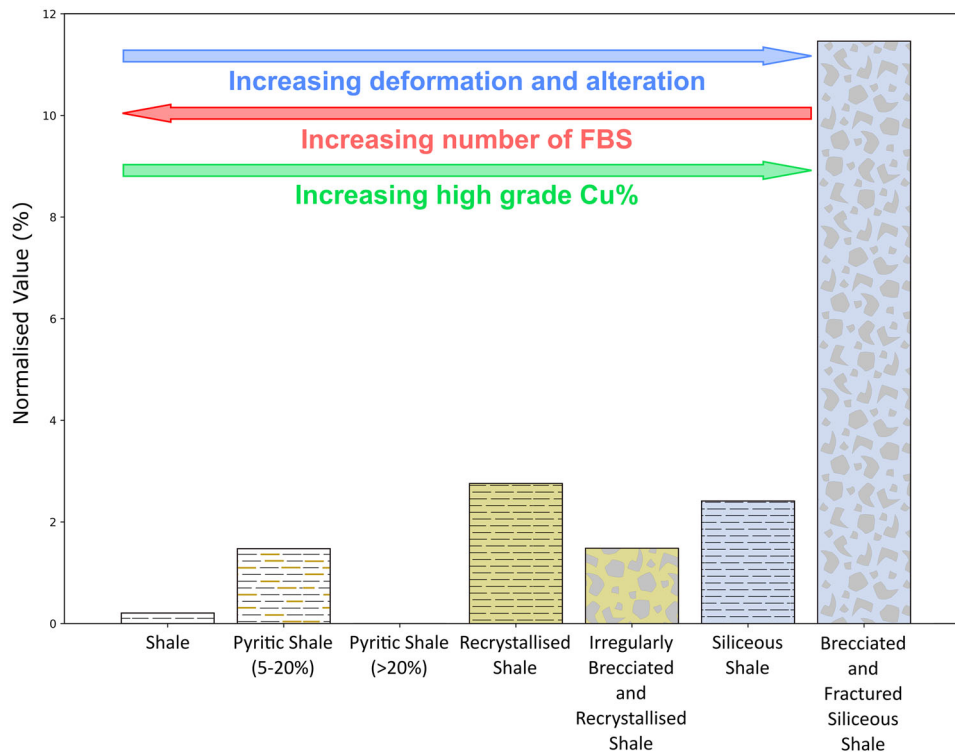


Figure 13. Lengths of drill-core intervals with ore-grade Cu (>3 wt% Cu) normalised to the total lengths of each lithology in the studied drill holes. The plot shows a strong correlation between ore-grade Cu and alteration and deformation.

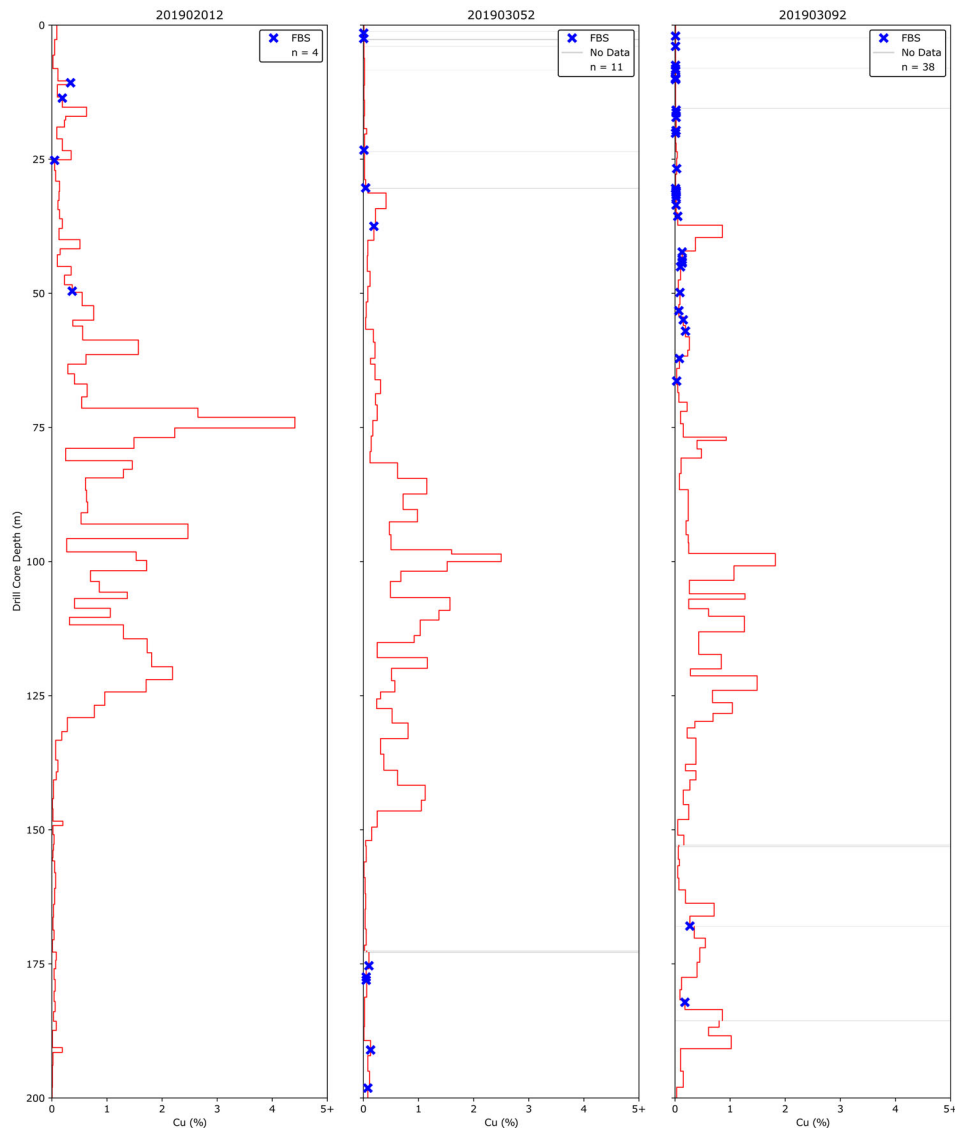


Figure 14. Downhole logs of Cu wt% in three MICO drill holes showing the locations of foliation boudinage structures and associated Cu wt%. Foliation boudinage structures are predominantly located in drill-hole intervals with the lowest Cu wt%.

may intersect large-scale foliation boudinage structures that are indistinguishable on the drill core scale from structures such as breccia, recrystallisation or veins. Foliation boudinage structures larger than the drill core diameter could be distinguished by the bending of bedding adjacent to these zones, but this is difficult to assess without orientated drill core close to the Cu ore bodies.

Currently, foliation boudinage structures have only been found at Mount Isa mine. However, they may exist at other deposits, and a search for their distribution at other Pb–Zn and Cu deposits in the area would allow their evaluation as a possible vector to ore.

### **Structural measurements and timing of foliation boudinage structures**

The most common foliation boudinage structures observed at Mount Isa are the asymmetrical x-type of Arslan *et al.*

(2008; Figures 9 and 10). Asymmetrical foliation boudinage structures can form in both simple and pure shear conditions, depending on initial fracture geometries (Figure 6). The asymmetrical structures at Mount Isa are likely to have formed through simple shear from fractures sub-perpendicular to bedding. Asymmetrical x-type foliation boudinage structures, which open into fluid filled voids and form by simple shear, can have many initial fracture geometries compared to those forming by pure shear, which require a specific sigmoidal-shaped fracture to form (Figure 6; Arslan *et al.*, 2008). It is considered unlikely that all foliation boudinage structures at Mount Isa formed by pure shear from fractures with this specific geometry. Therefore, it is more likely the asymmetrical foliation boudinage structures formed by simple shear of fractures with various orientations.

The necks of foliation boudinage structures are shown to have both north and south plunges in the same drill core independently of depth (Figure 11), implying that the

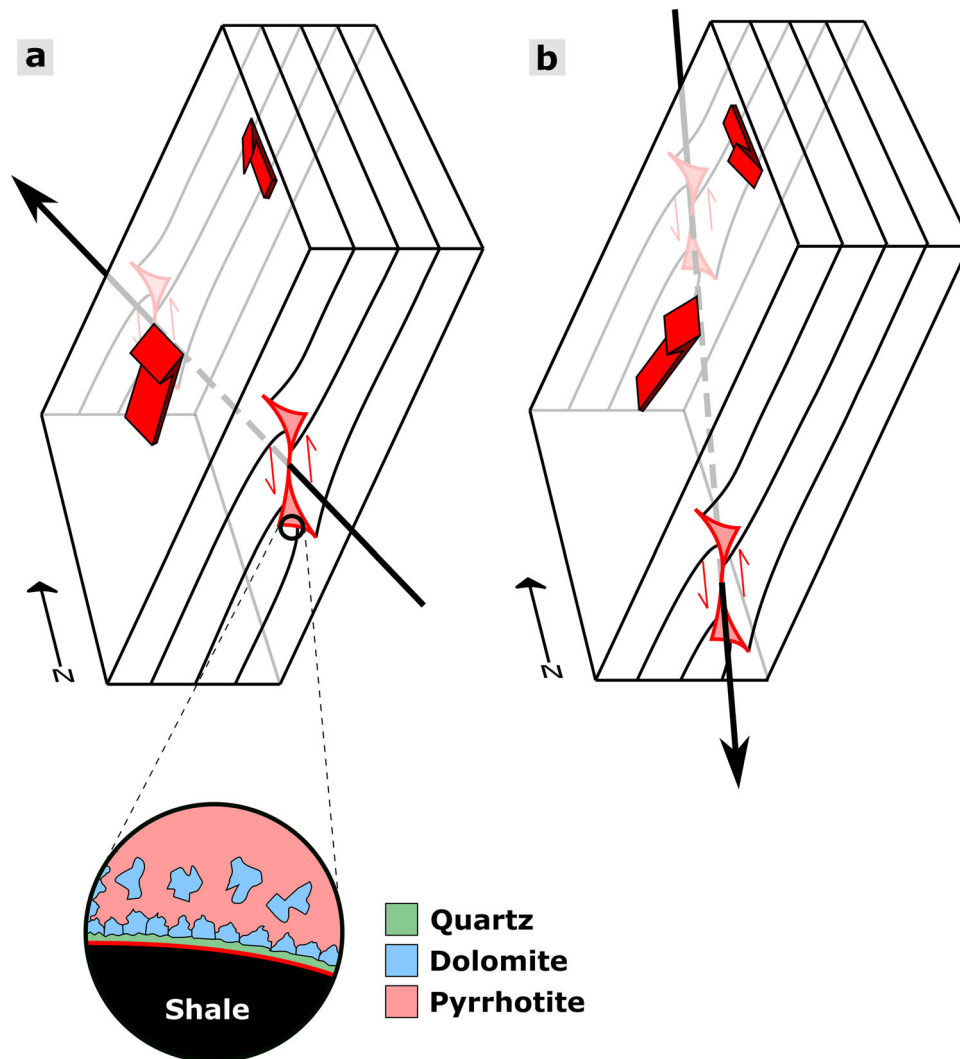


**Figure 15.** The formation of asymmetrical foliation boudinage structures at Mount Isa by approximately east–west shortening and up-dip, layer-parallel extension, showing the long axis of the foliation boudinage structures: (a) plunging to the north as a result of east–west shortening and dextral-reverse shear during D4a; and (b) plunging to the south as a result of east–west shortening and sinistral-reverse shear during D4b. Red arrows at foliation boudinage structures show relative displacements of the fracture walls. An enlarged diagram of the foliation boudinage structure infilling shows the initial quartz rim and subsequent dolomite, with later sulfide (pyrrhotite ± chalcopyrite) infill and replacement.

plunge directions are not domainal in the deposit. The long axes of foliation boudinage structures lie on the great circles of the Urquhart Shale bedding planes (Figure 11; Supplemental data, Figure S1). This relationship is preserved as the orientation of the bedding changes along the drill hole. Therefore, the shale bedding or a bedding-parallel foliation must be the controlling fabric anisotropy in the development of the foliation boudinage structures at Mount Isa. The homogeneous nature of the Urquhart Shale and anisotropy provided by the fine lamination favours the formation of foliation boudinage structures.

The north–south orientations of the foliation boudin long axes indicate the intermediate principal strain axis during their formation (Arslan *et al.*, 2008) and when combined with the steep orientation of the anisotropy, show approximate east–west shortening (Figure 15). The deformation history at Mount Isa is complex (Bell *et al.*, 1988; Davis, 2004; Miller, 2007) with D2, D3, D4a, the D4b syn-Cu

event of Miller (2007), D5a and D5b all corresponding to approximately east–west shortening.

The D5a and D5b events are shown by Miller (2007) to have post-silica-dolomite, pyrrhotite and Cu mineralisation timings and therefore they also have a post-foliation boudin timing. Some of the deformation events with an east–west shortening may be compatible, however, a protracted period of foliation boudin formation is favoured based on their north and south plunges. The variation in the plunge of the foliation boudinage structures is interpreted to reflect an evolution from D4a through to the D4b syn-Cu event. The east-northeast–west-southwest shortening of the steeply west-dipping Urquhart Shale during D4a resulted in dextral-reverse shear along bedding surfaces with a top to the northeast shear direction (Figure 15a). Foliation boudinage structures formed as a result of this deformation have long axes that plunge to the north (Figure 15a). Miller's (2007) unnamed northwest–southeast



shortening sinistral-reverse shear event (D4b), which he interprets as having a syn-Cu mineralisation timing, has a top to the southeast shear direction and resulted in foliation boudinage structures plunging to the south (Figure 15b).

All foliation boudinage structures in this study have sulfide infills of pyrrhotite ± chalcopyrite. The foliation boudinage structures have an identical mineral paragenesis to the rest of the deposit (e.g. Cave *et al.*, 2020; Perkins, 1984) and no evidence has been found in this study to suggest the silica-dolomite + pyrrhotite ± chalcopyrite infills of the foliation boudinage structures have been remobilised and precipitated at a later stage. This agrees with the observations of Perkins (1984) that, once precipitated, chalcopyrite does not redissolve and reprecipitate.

Arslan *et al.* (2008) stated that a high fluid pressure is critical for the formation of foliation boudinage structures and in maintaining open fluid-filled fractures. High fluid pressures during the silica-dolomite alteration could be a contributing factor to the formation of foliation boudinage structures at Mount Isa. The drop in fluid pressure during the brecciation (Bell *et al.*, 1988; Perkins, 1984) may have resulted in the cessation of silica-dolomite, pyrrhotite and minor chalcopyrite infilling of the foliation boudinage structures. The initial infill was followed by continuing pyrrhotite ± chalcopyrite replacement of the silica-dolomite within the foliation boudinage structures during the Cu brecciation event.

The results in this study largely support Miller's (2007) unnamed sinistral-reverse (D4b) timing for Cu brecciation at the Mount Isa deposit. However, a prolonged Cu mineralisation episode from late-D4a through to the main Cu brecciation during D4b is favoured based on the infill characteristics of the foliation boudinage structures. A Cu mineralisation event that initiates in late D4a and progresses through to the main Cu brecciation and mineralisation event in D4b would show an initial infill and then replacement of silica-dolomite in both the north and south plunging structures. However, a similar infill could be observed in foliation boudinage structures by a Cu event restricted to D4b if the D4b south-plunging structures were infilled and the D4a north-plunging structures were largely mineralised by replacement of the existing silica-dolomite infill.

## Conclusions

- Petrographic analysis at the Mount Isa Cu deposit shows that foliation boudinage structures in drill core have an infill of quartz, dolomite and pyrrhotite, with minor chalcopyrite in some samples. Pyrrhotite replaces and infills around quartz and dolomite in all analysed samples. Chalcopyrite has a coeval or post-pyrrhotite timing.
- The foliation boudinage structures plunge gently to the north and south as a result of layer normal shortening and layer parallel extension of the steeply west-dipping Urquhart Shale.
- Drill core-scale foliation boudinage structures at Mount Isa are identified almost exclusively within the unaltered and undeformed Urquhart Shale and 'pyritic shale (5–20% pyrite)' lithologies, where the anisotropy required for their formation was still intact. The homogeneous nature of the Urquhart Shale at the small scale, combined with the anisotropy provided by the shale layering or layer-parallel foliation, was conducive to the formation of foliation boudinage structures at Mount Isa.
- The drill core-scale foliation boudinage structures are generally located outside the zone of high-grade Cu mineralisation, although within the silica-dolomite and pyrrhotite mineralisation halos.
- Foliation boudinage structures formed after dolomitisation and silicification along bedding. Infilling of the structures occurred during a protracted silica-dolomite, pyrrhotite and chalcopyrite mineralisation event. The paragenesis of the foliation boudinage structures is consistent with the established paragenesis of the main Cu mineralisation at Mount Isa.
- The orientations and mineral infills show a continued formation of foliation boudinage structures from east-northeast–west-southwest dextral-reverse shortening during D4a through to the main Cu mineralisation during Miller's (2007) unnamed west-northwest–east-southeast sinistral-reverse shortening event (D4b).

## Acknowledgements

We thank Anthony Oldroyd for his expertise in producing polished thin sections and Duncan Muir with SEM mineral phase analysis. We thank all the staff at Mount Isa Mines for their assistance during the data collection and for facilitating the research project. We also thank Alex Brown, Ollie Campbell and Levent Tosun for their inciteful comments, and Julian Vearncombe and Nick Hayward for their detailed reviews in improving the manuscript.

## Disclosure statement

No potential conflict of interest was reported by the author(s).

## Funding

BJW is supported by a NERC GW4+ Doctoral Training Partnership studentship from the Natural Environment Research Council [NE/L002434/1] and is thankful for the support and additional funding from CASE partner, Mount Isa Mines Ltd.

## ORCID

B. J. Williams  <http://orcid.org/0000-0002-0576-657X>  
 T. G. Blenkinsop  <http://orcid.org/0000-0001-9684-0749>  
 R. Lilly  <http://orcid.org/0000-0001-9111-2056>

## Data availability statement

Tables S1 and S2 and Figures S1 and S2 are included as supplemental data.

## References

- Aerden, D. G. A. (1991). Foliation-boudinage control on the formation of the Rosebery Pb–Zn orebody. *Journal of Structural Geology*, 13(7), 759–775. [https://doi.org/10.1016/0191-8141\(91\)90002-Z](https://doi.org/10.1016/0191-8141(91)90002-Z)
- Andrew, B. S. (2020). *Recognising cryptic alteration surrounding the Mount Isa Copper Deposits: Implications for controls on fluid flow, and mineral exploration* [Unpublished PhD thesis]. University of Waikato.
- Arslan, A., Koehn, D., Passchier, C. W., & Sachau, T. (2012). The transition from single layer to foliation boudinage: A dynamic modelling approach. *Journal of Structural Geology*, 42, 118–126. <https://doi.org/10.1016/j.jsg.2012.06.005>
- Arslan, A., Passchier, C. W., & Koehn, D. (2008). Foliation boudinage. *Journal of Structural Geology*, 30(3), 291–309. <https://doi.org/10.1016/j.jsg.2007.11.004>
- Bell, T. H. (1983). Thrusting and duplex formation at Mount Isa, Queensland, Australia. *Nature*, 304(5926), 493–497. <https://doi.org/10.1038/304493a0>
- Bell, T. H. (1991). The role of thrusting in the structural development of Mount Isa mine and its implications for exploration in the surrounding region. *Economic Geology*, 86(8), 1602–1625. <https://doi.org/10.2113/gsecongeo.86.8.1602>
- Bell, T. H., & Hickey, K. A. (1998). Multiple deformations with successive subvertical and subhorizontal axial planes in the Mount Isa Region; Their impact on geometric development and significance for mineralization and exploration. *Economic Geology*, 93(8), 1369–1389. <https://doi.org/10.2113/gsecongeo.93.8.1369>
- Bell, T. H., Perkins, W. G., & Swager, C. P. (1988). Structural controls on development and localization of syntectonic copper mineralization at Mount Isa, Queensland. *Economic Geology*, 83(1), 69–85. <https://doi.org/10.2113/gsecongeo.83.1.69>
- Betts, P. G., Giles, D., Mark, G., Lister, G. S., Goleby, B. R., & Aillères, L. (2006). Synthesis of the Proterozoic evolution of the Mt Isa Inlier. *Australian Journal of Earth Sciences*, 53(1), 187–211. <https://doi.org/10.1080/08120090500434625>
- Betts, P. G., Lister, G. S., & O’Dea, M. G. (1998). Asymmetric extension of the middle Proterozoic lithosphere, Mount Isa terrane, Queensland, Australia. *Tectonophysics*, 296(3–4), 293–316. [https://doi.org/10.1016/S0040-1951\(98\)00144-9](https://doi.org/10.1016/S0040-1951(98)00144-9)
- Betts, P. G., Lister, G. S., & Pound, K. S. (1999). Architecture of a Palaeoproterozoic rift system: evidence from the Fiery Creek Dome region, Mt Isa terrane. *Australian Journal of Earth Sciences*, 46(4), 533–554. <https://doi.org/10.1046/j.1440-0952.1999.00721.x>
- Blake, D. H. (1987). Geology of the Mount Isa Inlier and environs, Queensland and Northern Territory. *Bureau of Mineral Resources Geology & Geophysics Bulletin*, 225, 83. [https://d28rz98at9flks.cloudfront.net/21/Bull\\_225.pdf](https://d28rz98at9flks.cloudfront.net/21/Bull_225.pdf)
- Blake, D. H., & Stewart, A. J. (1992). Stratigraphy and tectonic framework, Mount Isa Inlier. *Australian Geological Survey Organisation Bulletin*, 243, 1–11.
- Blenkinsop, T., Doyle, M., & Nugus, M. (2015). A unified approach to measuring structures in orientated drill core. *Geological Society, London, Special Publications*, 421(1), 99–108. <https://doi.org/10.1144/SP421.1>
- Cave, B., Lilly, R., & Barovich, K. (2020). Textural and geochemical analysis of chalcopyrite, galena and sphalerite across the Mount Isa Cu to Pb–Zn transition: Implications for a zoned Cu–Pb–Zn system. *Ore Geology Reviews*, 124, 103647. <https://doi.org/10.1016/j.oregeorev.2020.103647>
- Clark, G. J. (1968). *A mineralogical examination of the 1100 copper orebody*. Unpublished internal company report of Mount Isa Mines Limited.
- Connors, K. A., & Page, R. W. (1995). Relationships between magmatism, metamorphism and deformation in the western Mount Isa Inlier, Australia. *Precambrian Research*, 71(1–4), 131–153. [https://doi.org/10.1016/0301-9268\(94\)00059-Z](https://doi.org/10.1016/0301-9268(94)00059-Z)
- Davis, T. P. (2004). Mine-scale structural controls on the Mount Isa Zn–Pb–Ag and Cu orebodies. *Economic Geology*, 99(3), 543–559. <https://doi.org/10.2113/gsecongeo.99.3.543>
- Day, R. W., Whitaker, W. G., Murray, C. G., Wilson, I. H., & Grimes, K. G. (1983). *Queensland geology. A companion volume to the 1:2 500 000 scale geological map (1975)*. Geological Survey of Queensland, Publication 383.
- Domagala, J., Southgate, P. N., Mc Conachie, B. A., & Pidgeon, B. A. (2000). Evolution of the Palaeoproterozoic Prize, Gun and lower Loretta Supersequences of the Surprise Creek Formation and Mt Isa Group. *Australian Journal of Earth Sciences*, 47(3), 485–507. <https://doi.org/10.1046/j.1440-0952.2000.00796.x>
- Duncan, R. J., Wilde, A. R., Bassano, K., & Maas, R. (2006). Geochronological constraints on tourmaline formation in the Western Fold Belt of the Mount Isa Inlier, Australia: Evidence for large-scale metamorphism at 1.57 Ga? *Precambrian Research*, 146(3–4), 120–137. <https://doi.org/10.1016/j.precamres.2006.01.010>
- Glencore. (2022). *Mount Isa mines*. <https://www.glencore.com.au/operations-and-projects/qld-metals/operations/mount-isa-mines>
- Goscombe, B. D., Passchier, C. W., & Hand, M. (2004). Boudinage classification: End-member boudin types and modified boudin structures. *Journal of Structural Geology*, 26(4), 739–763. <https://doi.org/10.1016/j.jsg.2003.08.015>
- Gulson, B. L., Perkins, W. G., & Mizon, K. J. (1983). Lead isotope studies bearing on the genesis of copper orebodies at Mount Isa, Queensland. *Economic Geology*, 78(7), 1466–1504. <https://doi.org/10.2113/gsecongeo.78.7.1466>
- Hambrey, M. J., & Milnes, A. G. (1975). Boudinage in glacier ice — some examples. *Journal of Glaciology*, 14(72), 383–393. <https://doi.org/10.1017/S0022143000021912>
- Jackson, M. J., Scott, D. L., & Rawlings, D. J. (2000). Stratigraphic framework for the Leichhardt and Calvert Superbasins: Review and correlations of the pre- 1700 Ma successions between Mt Isa and McArthur River. *Australian Journal of Earth Sciences*, 47(3), 381–403. <https://doi.org/10.1046/j.1440-0952.2000.00789.x>
- Knights, J. G. (1976). *The 1100 orebody from zero to 1000 m*. Unpublished internal company report of Mount Isa Mines Ltd.
- Large, R. R., Bull, S. W., McGoldrick, P. J., Walters, S., Derrick, G. M., Carr, G. R. (2005). Stratiform and strata-bound Zn–Pb–Ag deposits in Proterozoic sedimentary basins, Northern Australia. In *One Hundredth Anniversary Volume: Vol. Economic Geology* (pp. 931–963). Society of Economic Geologists. <https://doi.org/10.5382/AV100.28>
- Large, R. R., Bull, S. W., Selley, D., Yang, J., Cooke, D., Garven, G., & McGoldrick, P. J. (2002). Controls on the formation of giant stratiform sediment-hosted Zn–Pb–Ag deposits: With particular reference to the north Australian Proterozoic. In D. R. Cooke & J. Pongratz (Eds.), *Giant ore deposits: Characteristics, genesis and exploration* (pp. 107–150). CODES Special Publication 4, University of Tasmania.
- Long, R. D. (2010). *The Paroo Fault and the Mount Isa Copper Orebodies: A revised structural and evolutionary model, Mt Isa, Queensland, Australia* [Unpublished PhD thesis]. James Cook University.
- Mandal, N., & Karmakar, S. (1989). Boudinage in homogeneous foliated rocks. *Tectonophysics*, 170(1–2), 151–158. [https://doi.org/10.1016/0040-1951\(89\)90109-1](https://doi.org/10.1016/0040-1951(89)90109-1)
- Mathias, B. V., & Clark, G. J. (1975). Mount Isa copper and silver–lead–zinc orebodies. Isa and Hilton mines. In C. L. Knight (Ed.), *Economic geology of Australia and Papua New Guinea, I. Metals* (pp. 351–371). Australasian Institute of Mining and Metallurgy Monograph 5.
- Miller, J. M. (2007). *Structural controls on the Mount Isa Copper deposit, QLD*. pmd\*CRP Project i7 – Project I7 Final Report.
- Milnes, A. G. (1964). *Structure and history of the Antigorite nappe (Simplon group) north Italy* [Unpublished PhD thesis]. University of Basel.
- Neudert, M. K. (1983). *A depositional model for the Upper Mount Isa Group and implications for ore formation* [Unpublished PhD thesis]. Australian National University.
- Neumann, N. L., Southgate, P. N., Gibson, G. M., & MCintyre, A. (2006). New SHRIMP geochronology for the Western Fold Belt of the Mt Isa Inlier: Developing a 1800 – 1650 Ma event framework. *Australian*

- Journal of Earth Sciences*, 53(6), 1023–1039. <https://doi.org/10.1080/08120090600923287>
- O'Dea, M. G., & Lister, G. S. (1995). The role of ductility contrast and basement architecture in the structural evolution of the Crystal Creek block, Mount Isa Inlier, NW Queensland, Australia. *Journal of Structural Geology*, 17(7), 949–960. [https://doi.org/10.1016/0191-8141\(94\)00117-1](https://doi.org/10.1016/0191-8141(94)00117-1)
- O'Dea, M. G., Lister, G. S., Betts, P. G., & Pound, K. S. (1997). A shortened intraplate rift system in the Proterozoic Mount Isa terrane, NW Queensland, Australia. *Tectonics*, 16(3), 425–441. <https://doi.org/10.1029/96TC03276>
- O'Dea, M. G., Lister, G. S., Maccready, T., Betts, P. G., Oliver, N. H. S., Pound, K. S., Huang, W., Valenta, R. K., Oliver, N. H. S., & Valenta, R. K. (1997). Geodynamic evolution of the Proterozoic Mount Isa Terrain. *Geological Society, London, Special Publications*, 121(1), 99–122. <https://doi.org/10.1144/GSL.SP.1997.121.01.05>
- Page, R. W. (1983). Timing of superposed volcanism in the Proterozoic Mount Isa Inlier, Australia. *Precambrian Research*, 21(3–4), 223–245. [https://doi.org/10.1016/0301-9268\(83\)90042-6](https://doi.org/10.1016/0301-9268(83)90042-6)
- Page, R. W., & Bell, T. H. (1986). Isotopic and structural responses of granite to successive deformation and metamorphism. *The Journal of Geology*, 94(3), 365–379. <https://doi.org/10.1086/629035>
- Page, R. W., Jackson, M. J., & Krassay, A. A. (2000). Constraining sequence stratigraphy in north Australian basins: SHRIMP U–Pb zircon geochronology between Mt Isa and McArthur river. *Australian Journal of Earth Sciences*, 47(3), 431–459. <https://doi.org/10.1046/j.1440-0952.2000.00797.x>
- Page, R. W., & Sun, S. S. (1998). Aspects of geochronology and crustal evolution in the Eastern Fold Belt, Mt Isa Inlier. *Australian Journal of Earth Sciences*, 45(3), 343–361. <https://doi.org/10.1080/08120099808728396>
- Page, R. W., & Sweet, I. P. (1998). Geochronology of basin phases in the western Mt Isa Inlier, and correlation with the McArthur Basin. *Australian Journal of Earth Sciences*, 45(2), 219–232. <https://doi.org/10.1080/08120099808728383>
- Page, R. W., & Williams, I. S. (1988). Age of the Barramundi Orogeny in northern Australia by means of ion microprobe and conventional U–Pb zircon studies. *Precambrian Research*, 40–41, 21–36. [https://doi.org/10.1016/0301-9268\(88\)90059-9](https://doi.org/10.1016/0301-9268(88)90059-9)
- Perkins, C., Heinrich, C. A., & Wyborn, L. A. I. (1999). <sup>40</sup>Ar/<sup>39</sup>Ar geochronology of copper mineralization and regional alteration, Mount Isa, Australia. *Economic Geology*, 94(1), 23–36. <https://doi.org/10.2113/gsecongeo.94.1.23>
- Perkins, W. G. (1984). Mount Isa Silica Dolomite and Copper orebodies; The result of a syntectonic hydrothermal alteration system. *Economic Geology*, 79(4), 601–637. <https://doi.org/10.2113/gsecongeo.79.4.601>
- Perkins, W. G. (1997). Mount Isa lead–zinc orebodies: Replacement lodes in a zoned syndeformational copper–lead–zinc system? *Ore Geology Reviews*, 12(2), 61–110. [https://doi.org/10.1016/S0169-1368\(97\)00004-8](https://doi.org/10.1016/S0169-1368(97)00004-8)
- Platt, J. P., & Vissers, R. L. M. (1980). Extensional structures in anisotropic rocks. *Journal of Structural Geology*, 2(4), 397–410. [https://doi.org/10.1016/0191-8141\(80\)90002-4](https://doi.org/10.1016/0191-8141(80)90002-4)
- Potgieter, G. S. (2015). Work conducted in preparation for partial extraction of X41 shaft pillar at Mount Isa Mines. In Y. Potvin (Ed.), *Design methods 2015: Proceedings of the international seminar on design methods in underground mining* (pp. 273–290). Australian Centre for Geomechanics. [https://doi.org/10.36487/ACG\\_rep/1511\\_15\\_Potgieter](https://doi.org/10.36487/ACG_rep/1511_15_Potgieter)
- Rubenach, M. J. (1992). Proterozoic low-pressure/high-temperature metamorphism and an anticlockwise P–T–t path for the Hazeldene area, Mount Isa Inlier, Queensland, Australia. *Journal of Metamorphic Geology*, 10(3), 333–346. <https://doi.org/10.1111/j.1525-1314.1992.tb00088.x>
- Sawyer, E. W. (1983). The structural history of a part of the Archaean Quetico Metasedimentary Belt, superior province, Canada. *Precambrian Research*, 22(3–4), 271–294. [https://doi.org/10.1016/0301-9268\(83\)90052-9](https://doi.org/10.1016/0301-9268(83)90052-9)
- Scott, D. L., Rawlings, D. J., Page, R. W., Tarlowski, C. Z., Idnurm, M., Jackson, M. J., & Southgate, P. N. (2000). Basement framework and geodynamic evolution of the Palaeoproterozoic superbasins of north-central Australia: An integrated review of geochemical, geochronological and geophysical data Basement framework and geodynamic. *Australian Journal of Earth Sciences*, 47(3), 341–380. <https://doi.org/10.1046/j.1440-0952.2000.00793.x>
- Smith, J. W., Burns, M. S., & Croxford, N. J. W. (1978). Stable isotope studies of the origins of mineralization at Mount Isa. I. *Mineralium Deposita*, 13(3), 369–381. <https://doi.org/10.1007/BF00206570>
- Southgate, P. N., Bradshaw, B. E., Domagala, J., Jackson, M. J., Idnurm, M., Krassay, A. A., Page, R. W., Sami, T. T., Scott, D. L., Lindsay, J. F., McConachie, B. A., & Tarlowski, C. (2000). Chronostratigraphic basin framework for Palaeoproterozoic rocks (1730–1575 Ma) in northern Australia and implications for base-metal mineralisation. *Australian Journal of Earth Sciences*, 47(3), 461–483. <https://doi.org/10.1046/j.1440-0952.2000.00787.x>
- Spatial and Graphic Services Statewide Operations Department of Natural Resources Mines and Energy. (2020). *Mount Isa Surface Geology*. Geological Survey of Queensland. <https://geoscience.data.qld.gov.au/data/map-collection/mr009838>
- Swager, C. P. (1985). Syndeformational carbonate-replacement model for the copper mineralization at Mount Isa, Northwest Queensland: A microstructural study. *Economic Geology*, 80(1), 107–125. <https://doi.org/10.2113/gsecongeo.80.1.107>
- Swager, C. P., Perkins, W. G., & Knights, J. G. (1987). Stratabound phyllosilicate zones associated with syntectonic copper orebodies at Mt Isa, Queensland. *Australian Journal of Earth Sciences*, 34(4), 463–476. <https://doi.org/10.1080/08120098708729426>
- Swanson, M. T. (1992). Late Acadian-Alleghenian transpressional deformation: Evidence from asymmetric boudinage in the Casco Bay area, coastal Maine. *Journal of Structural Geology*, 14(3), 323–341. [https://doi.org/10.1016/0191-8141\(92\)90090-J](https://doi.org/10.1016/0191-8141(92)90090-J)
- Terzaghi, R. D. (1965). Sources of error in joint surveys. *Géotechnique*, 15(3), 287–304. <https://doi.org/10.1680/geot.1965.15.3.287>
- Vearncombe, J., & Vearncombe, S. (1998). Structural data from drill core. In B. Davis & S. Ho (Eds.), *More meaningful sampling in the mining industry* (pp. 67–82). Australian Institute of Geoscientists, Bulletin 22.
- Wallis, I., Rowland, J., Dempsey, D., Allan, G., Sidik, R., Martikno, R., McLean, K., Sihotang, M., Azis, H., & Baroek, M. (2020). Approaches to imaging feedzone diversity with case studies from Sumatra, Indonesia and the Taupō Volcanic Zone, New Zealand. *Proceedings 42nd New Zealand Geothermal Workshop, Waitangi, New Zealand*.
- Waring, C. L. (1990). *Genesis of the Mount Isa Cu ore system* [Unpublished PhD thesis]. Monash University.
- Wiest, J. D., Fossen, H., & Jacobs, J. (2020). Shear zone evolution during core complex exhumation – Implications for continental detachments. *Journal of Structural Geology*, 140, 104139. <https://doi.org/10.1016/j.jsg.2020.104139>
- Wilde, A. R. (2011). Mount Isa copper orebodies: Improving predictive discovery. *Australian Journal of Earth Sciences*, 58(8), 937–951. <https://doi.org/10.1080/08120099.2011.571285>
- Wilde, A. R., Jones, P. A., Gessner, K., Aillères, L., Gregory, M. J., & Duncan, R. J. (2006). A geochemical process model for the Mount Isa copper orebodies. *Economic Geology*, 101(8), 1547–1567. <https://doi.org/10.2113/gsecongeo.101.8.1547>
- Winsor, C. N. (1986). Intermittent folding and faulting in the Lake Moondarra area, Mount Isa, Queensland. *Australian Journal of Earth Sciences*, 33(1), 27–42. <https://doi.org/10.1080/08120098608729348>